

低エネルギー陽子の照射による中性子の 生物影響のメカニズム研究

(課題番号：17310034)

平成17～19年度科学研究費補助金（基盤研究（B））
研究成果報告書



平成20年3月

研究代表者： 星 正 治
(広島大学原爆放射線医科学研究所 教授)

低エネルギー陽子の照射による中性子の 生物影響のメカニズム研究

目 次

はしがき	1
研究組織	3
研究経費	3
研究発表	5
研究成果	1 3

はしがき

広島大学原爆放射線医科学研究所には平成3年度より平成5年度までの間に、中性子の生物影響を研究する目的で、中性子発生装置が導入された（定価約5億円）。すでに本年は平成20年であるので完成してから15年経過した、本研究が始まった際もすでに10年以上経過していた。当初、中性子発生装置の本体は、3MeVのシェンケル型加速器である。この加速器で主に陽子（重陽子、アルファ線も可能）を加速する。目的とする中性子の発生は、リチウムターゲットへの陽子を当てることによってLi(p, n)反応により中性子を発生させる。この中性子は単色で0.1-1.2MeVの範囲のエネルギーを持つ。この加速器の電流は最大で1mAで、その際の線量率は30cGy/minである。設計に際して生物照射のためには短時間の照射が必要であり、想定されるあらゆる実験系に対し30分から1時間以内に照射が完了できることを目標とした。この装置は少なくとも日本で初めて建設された装置であったこともあり、その後1年間強は調整のための作業が中心であった。平成7年度から本格的な生物影響研究が開始された。しかし、10年経過するにつれ、加速管、イオン源などの消耗が見られるようになった。今回は特に本研究が開始されてまもなく、問題が発生し、本研究所のすべての放射線発生装置が2年近く運転を自粛したので、主に実験の場所は筑波大学加速器センターの2MVのタンデトロン(タンデム)加速器で行った。

現実に業務を行っている原子炉や、原爆被爆者で、東海村の被曝などで、実際に被曝の可能性のあるエネルギー領域は、0.1-1.2MeVである。原爆などの場合は2MeVを中心とし幅を持ったエネルギーであり、その影響が論じられている。またこのエネルギー領域では、放射線防護の分野の知識では中性子の生物影響が大きく変わるとされている。したがって、このエネルギー領域で“単色可変な”かつ、“生物実験のできる大線量の”中性子発生装置が求められていた。

中性子の生物影響研究を進める上で重要なことは、中性子の線量とエネルギースペクトルを正確に知ることである。このうち線量は対チェンバー法で正確に決定することができた。しかしながらもう一つの要素であるエネルギースペクトルはヘリウム3カウンターによっていた。しかし、その方法は簡便ではあるが十分な正確さで決定できていなかった。文部省科学研究費補助金により、飛行時間法(Time of flight (TOF))で正確なエネルギースペクトルが決定できるようになった。またその後空気中への陽子の取り出しと照射のシステムが導入された。その後、カスケードイメージインテンシファイアを使って取り出された陽子の測定も行った。本研究については、筑波大学の加速器科学研究センターの2MVのタンデトロン加速器を使って、陽子線を空気中に取り出し、外装チェンバーとシリコンサーフェスバリアー型半導体検出器で細胞レベルの放射線量測定の基礎を考察することにした。

ところで単色エネルギーの中性子の発生源を製作し生物影響研究を推進する理由はいくつかある。主なものをあげると、(1)中性子はガンマ線や電子線と比べると高い生物影響

がある。これを高 LET の放射線であるという。そのためふつうの放射線と比べることにより放射線の生物影響の初期過程でなにが起こるのか、そのメカニズムの解明に役に立つ。

(2) 広島原爆の中性子のエネルギーは長崎よりも低いと言われているが、もし影響がエネルギーによって違うなら広島長崎の被爆者への放射線の影響を考え直すことにつながる。

(3) 中性子の生物影響を理解する事は、中性子を取り扱っている作業従事者などへのリスクを知ることになる。これは安全な作業を行う基準となる。

中性子の生物影響 (Relative Biological Effectiveness (RBE)) の定義は、同じ生物影響を与えるガンマ線と中性子線の線量の比である。それが、場合によって 7 から 8 と大きいことがある。ときには 20 にもなることがある。この理由がよく分かっていない。中性子の線量の 70 - 80% は、生物主要成分である水素に中性子が衝突し、その水素の原子核 (陽子) が走ることによって生じる。しかしこの陽子そのものは、RBE が 1.0 - 1.2 ぐらいにしかならず説明が困難である。この点については、理論的計算によりその説明を試みた。また、本研究では細胞レベルの放射線量測定をすすめ、その線量の評価方法について検討し有効であることを確かめた。

後半では、理論計算に基づいた細胞レベルでの陽子線照射を行った際にその RBE がどのように変化するか の考察についてロシアの研究者との共同研究で行った考察を示す。

研究組織

研究代表者： 星 正 治

(広島大学原爆放射線医科学研究所 教授)

研究分担者： 遠 藤 暁 (広島大学原爆放射線医科学研究所 准教授)

田中 憲一 (広島大学原爆放射線医科学研究所 助教)

鬼塚 昌彦 (九州大学医学部 教授)

神谷 研二 (広島大学原爆放射線医科学研究所 教授)

檜枝光太郎 (立教大学理学部 教授)

上原 周三 (九州大学医学部 教授)

大 瀧 慈 (広島大学原爆放射線医科学研究所 教授)

研究協力者： Igor Khvostunov (ロシア医学アカデミー放射線医学研究所)

笹 公 和 (筑波大学大学院数理物質科学研究科)

高辻 俊宏 (長崎大学環境科学部)

佐 藤 斉 (茨城県立医療大学保健医療学部)

長島 泰夫 (筑波大学)

研究経費

交付決定額 (配分額)

(金額単位：千円)

	直接経費	間接経費	合 計
平成17年度	6, 500	0	6, 500
平成18年度	4, 500	0	4, 500
平成19年度	4, 500	1,350	5, 850
総 計	15, 500	1,350	16, 850

研究発表

(1) 雑誌論文

1. Khvostunov I. K., Nikjoo, H., Hoshi, M., Uehara, S.: The microdosimetric consideration of RBE of low-energy protons on V79 cells // In the Proceedings of Sissakian Memorial Symposium <Problems of Biochemistry, Radiation and Space Biology> dedicated to the centenary of Academician N. M. Sissakian's birth, 24 - 27 January, 2007, Dubna, Russia, PP. 336-339.

以下、参考論文

1. 星 正治, 遠藤 暁: 新しい原爆線量評価体系DS02. 臨床技術講座, 日本放射線技術学会雑誌, 61 (8), 1087-1093, 2005.
2. 星 正治: 講演「世界における被ばくの実態」. HICARE講演会世界の放射線被ばくの現状を知る報告書. 20-41, 2005.
3. Endo, S., Tanaka, K., Ishikawa, M., Hoshi, M., Onizuka, Y., Takada, M., Yamaguchi, H., Hayabuchi, N., Maeda, N., Shizuma, K.: Microdosimetric evaluation of the 400 MeV/nucleon carbon beam at HIMAC. *Medical Physics*, 32 (12), 3843-3848, 2005.
4. Tanaka, K., Kobayashi, T., Bengua, G., Nakagawa, Y., Endo, S., and Hoshi, M.: TPD based evaluation of moderator characteristics for BNCT using ${}^7\text{Li}(p,n)$ neutrons at proton energy of 2.5 MeV. *Jpn. Jour. Med. Phys.*, 25 (Sup.3-1), 355-358, 2005.
5. Tanaka, K., Kobayashi, T., Bengua, G., Nakagawa, Y., Endo, S., and Hoshi, M.: Characteristics of BDE dependent on dose protocol and ${}^{10}\text{B}$ concentration for BNCT using near-threshold ${}^7\text{Li}(p,n){}^7\text{Be}$ direct neutrons. *Physics in Medicine and Biology*, 50, 167-177, 2005.
6. 石川正純, 平澤雅彦, 富谷武浩, 村山秀雄, 星 正治: 非侵襲的ホウ素濃度分布測定システムの基礎的検討. 医学物理, 第25巻, 1号, 3-12, 2005.

7. Endo, S., Tanaka, K., Ishikawa, M., Hoshi, M., Onizuka, Y., Takada, M., Hayabuchi, N., Maeda, N., Shizuma, K.: Microdosimetric evaluation of secondary fragments in Phantom produced by therapeutic 290 MeV/nucleon carbon beam at HIMAC. Proceedings of the 1st Asian Congress of Radiation Research, 181, 2005.
8. 遠藤 暁：講演「暮らしの中の放射線」。HICARE 講演会世界の放射線被ばくの現状を知る報告書。8-19, 2005.
9. 星 正治：新しい原爆放射線評価システムDS02と背景. 応用物理学会放射線分科会誌「放射線」, 32 (3), 126-136, 2006.
10. Yin, H., Ito, A., Bhattacharjee, D. & Hoshi, M.: A comparative study on the protective effects of 17 β -estradiol, biochanin A and bisphenol A on mammary gland differentiation and tumorigenesis in rats. *Indian Journal of Experimental Biology*, 44, 540-546, July 2006.
11. Endo, S., Hoshi, M., Takada, J., Takatsuji, T., Ejima, Y., Saigusa, S., Tachibana, A. and Sasaki, M. S.: Development, Beam Characterization and Chromosoma Effectiveness of X-rays of RBC Characteristic X-ray Generator. *J. Radiat. Res.*, 47 (2), 103-112, 2006.
12. Sasaki, M. S., Endo, S., Ejima, Y., Saito, I., Okamura, K., Oka, Y., Hoshi, M.: Effective Dose Equivalent of A-bomb Radiation in Hiroshima and Nagasaki as Assessed by Chromosomal Effectiveness of Spectrum Energy Photons and Neutrons. *Radiat. Environm. Biophys.*, 45, 79-91, 2006.
13. Tanaka, K., Kobayashi, T., Gerard, B., Nakagawa, Y., Endo, S and Hoshi, M.: Characterization of moderator assembly dimension for accelerator boron neutron capture therapy of brain tumors using $^7\text{Li}(p,n)$ neutrons at proton energy of 2.5 MeV., *Med. Phys.* 33: 1688-1694, 2006.
14. Tanaka, K., Kobayashi, T., Gerard, B., Nakagawa, Y., Endo, S and Hoshi, M.: Characterization indexes of moderator assembly for accelerator-based BNCT using $^7\text{Li}(p,n)$ neutrons at proton energy of 2.5 MeV., *Advances in Neutron Capture Therapy 2006 (Proceedings of 12th International Congress on Neutron Capture Therapy)*, 323-326, 2006.
15. 前田直子, 田原大世, 小西康彦, 村尾信夫, 島本茂利, 菅 慎治, 田中憲一, 遠藤 暁, 星 正治, 鬼塚昌彦, 早瀬尚文：MCNPモンテカルロコードを用いた ^{60}Co 照射装置のスペクトルと出力計算. 日本放射線腫瘍学会誌, 18 (4), 209-215, 2006.
16. Endo, S., Takada, M., Onizuka, Y., Tanaka, K., Maeda, N., Ishikawa, M., Miyahara, N., Hayabuchi, N., Shizuma, K. and Hoshi, M.: Microdosimetric Evaluation of Secondary Particles in a Phantom Produced by Carbon 290 MeV/Nucleon Ions at HIMAC. *J. Radiat. Res.*, 48 (5), 397-400, 2007.

17. Endo, S., Shizuma, K., Tanaka, K., Ishikawa, M., Ruhm, W., Egbert, S. D. and Hoshi, M.: Radioactivity in Atomic-Bomb Samples from Exposure to Environmental Neutrons. *Health Physics*, 93 (6), 689-695, 2007.
18. Endo, S., Tanaka, K., Fujikawa, K., Horiguchi, T., Itoh, T., Bengua, G., Nomura, T. and Hoshi, M.: Distortion of Neutron Field during Mice Irradiation at Kinki University Reactor UTR-KINKI. *Appl. Radiat. Isot.*, 65 (9), 1037-1040, 2007.
19. Endo, S., Tanaka, K., Takada, M., Onizuka, Y., Miyahara, N., Sato, T., Ishikawa, M., Maeda, N., Hayabuchi, N., Shizuma, K. and Hoshi, M.: Microdosimetric evaluation of secondary neutrons in a phantom produced by a 290 MeV/nucleon carbon beam at HIMAC. *Med. Phys.* 34 (9), 3571-3578, 2007.
20. Golikov, V., Wallstro, E., Wohni, T., Tanaka, K., Endo, S., Hoshi, M.: Evaluation of conversion coefficients from measurable to risk quantities for external exposure over contaminated soil by use of physical human phantoms. *Radiat. Environm. Biophys.* 46 (4), 375-382, 2007.
21. Kobayashi, T., Bengua, G., Tanaka, K. and Nakagawa, Y.: Variations in lithium target thickness and proton energy stability for the near-threshold ${}^7\text{Li}(p,n){}^7\text{Be}$ accelerator-based BNCT. *Physics in Medicine and Biology*, 52, 645-658, 2007.
22. Whitehead, N.E., Endo, S., Tanaka, K., Takatsuji, T., Hoshi, M., Fukutani, S., Ditchburn, R. G., Zondervan, A.: A preliminary study on the use of ${}^{10}\text{Be}$ in forensic radioecology. *J. Environ. Radio. Act.* 99, 260-270, 2008.

(2) 学会発表

1. 遠藤 暁：放射性同位元素の安全取扱 3－放射線発生装置，X 線発生装置，ECD ガスクロなどの安全取扱－。放射線業務従事者のための教育訓練講習会。広島，2005年5月13日。
2. 田中憲一，古林 徹，Gerard Bengua，中川義信，遠藤 暁，星 正治：2.5MeV 陽子による ${}^7\text{Li}(p,n)$ 反応を用いた加速器 BNCT 照射場の検討。第2回日本中性子捕捉療法研究会，筑波，7月，2005。
3. Tanaka, K., Kobayashi, T., Bengua, G., Nakagawa, Y., Endo, S. and Hoshi, M.: TPD based evaluation of moderator characteristics for BNCT using ${}^7\text{Li}(p,n)$ neutrons at proton energy of 2.5 MeV. 4th Japan-Korea Joint Meeting on Medical Physics, Kyoto, September, 2005.
4. Bengua, G., Tanaka, K., Kobayashi, T. and Nakagawa, Y.: Gaussian proton energy spectrum for BNCT using near threshold ${}^7\text{Li}(p,n){}^7\text{Be}$ neutrons. 4th Japan-Korea Joint Meeting on Medical Physics, Kyoto, September, 2005.
5. Onizuka, Y., Endo, S., Tanaka, K., Hoshi, M., Ishikawa, M., Sakurai, Y., Kobayahi, T., Hayabuchi, N., Takatsuji, T., Takada, M. and Maeda, N.: Measurement of radiation dose on lateral direction. 4th Japan-Korea Joint Meeting on Medical Physics, Kyoto, September, 2005.
6. Ishikawa, M., Kumada, H., Yamamoto, K., Kaneko, J., Sakurai, Y. and Tanaka, K.: Upgrade of scintillator with optical fiber detector using compensation of gamma ray and dead-time correction. 4th Japan-Korea Joint Meeting on Medical Physics, Kyoto, September, 2005.
7. 遠藤 暁：霧箱を使って放射線・宇宙線を見てみよう。青少年科学の祭典。広島，2005年11月13日。
8. Tanaka, K., Tieliewuhan, E., Endo, S., Toyoda, S., Romanyukha, A. and Hoshi, M.: Verification of Monte-Carlo-based conversion of imaging plate response for measurement of ${}^{90}\text{Sr}$ accumulation in teeth. 1st Asian Congress of Radiation Research, Hiroshima, November, 2005.
9. 星 正治：新しい原爆線量評価システムDS02 の背景とまとめ。特別講演。放射線取扱主任者部会年次大会，広島，2005年11月17日。
10. 田中憲一，広島大学原爆放射線医科学研究所線量測定・評価研究分野，広島大学大学院工学研究科量子エネルギー工学，広島大学原爆放射線医科学研究所国際放射線情報センター：広島原爆被ばく資料の紹介。放射線取扱主任者部会年次大会，広島，2005年11月17日。
11. 遠藤 暁：放射線の基礎知識－放射線の性質、単位、人体への影響－。緊急被ばく医療「島根

フォーラム」，松江，平成18年1月20日。

12. Whitehead, N.: How recoil sputtering affects the weathering of Chernobyl hot particles. 11th Hiroshima International Symposium -20th anniversary of the Chernobyl accident and related Semipalatinsk problems-. Hiroshima, February 7, 2006.
13. 星 正治：「密封線源の取扱及び施設の安全管理」。電子科学研究所放射線取扱主任者定期講習会講師，広島，平成18年3月9日。
14. 遠藤 暁：「非密封、放射線発生装置」。電子科学研究所放射線取扱主任者定期講習会講師，広島，平成18年3月9日。
15. 遠藤 暁：セミパラチンスク核実験場近郊線量評価とI-129 測定の提案。筑波大学加速器センターセミナー，筑波，平成18年3月17日。
16. 星 正治：新しい原爆放射線量評価システムDS02 の背景とまとめ。「広島・長崎原爆放射線量新評価システムDS02 と環境放射能計測技術」，2006年春季第53回応用物理学関係連合講演会，東京，平成18年3月23日。
17. 田中憲一，古林 徹，Bengua, G., 中川義信，遠藤 暁，星 正治：中性子捕捉療法 of 物理工学。日本原子力学会中国・四国支部第8回通常総会講演会，岡山，5月，2006。
18. Sahoo, S. K., Yonehara, H., Enomoto, H., Hoshi, M., Takada, J.: Measurement of Uranium Isotopes in Hiroshima “Black-Rain” Soil samples. 日本保健物理学会第40回研究発表会。広島，平成18年6月8日-9日。
19. 星 正治：日米共同研究による広島・長崎の原爆放射線の見積もりおよびセミパラチンスク核実験場周辺住民の被曝と健康影響。九州大学，福岡，平成18年7月4日。
20. 遠藤 暁：放射線を見る－簡易霧箱の作成－。日本原子力学会オープンスクール，広島，平成18年7月5日。
21. 遠藤 暁，豊田 新，小村和久，田中憲一，白石久二雄，今中哲二，西戸裕嗣，藤元憲三，明石真言，宮澤忠蔵，星 正治：JCO被ばく者歯中アマルガムを用いた中性子被ばく線量の推定。日本放射線影響学会第49回大会，札幌，平成18年9月6-8日。
22. 星 正治：放射線の計測Ⅱ 線量評価と事例（選択）。第1回緊急被ばく医療セミナー。千葉，平成18年9月20-21日。

23. 遠藤 暁, 鬼塚昌彦, 田中憲一, 高田真志, 前田直子, 宮原信幸, 早瀬尚文, 石川正純, 星 正治: 290MeV/核子炭素ビームが生成する中性2次フラグメントのマイクロドシメトリ. 日本医学物理学会第92回大会. 福岡, 平成18年9月29-30日.
24. Tanaka, K., Kobayashi, T., Gerard, B., Nakagawa, Y., Endo, S. and Hoshi, M.: Characterization indexes of moderator assembly for accelerator-based BNCT using ${}^7\text{Li}(p,n)$ neutrons at proton energy of 2.5 MeV, 12th International Congress on Neutron Capture Therapy, Kagawa, October 9-13, 2006.
25. Kobayashi, T., Bengua, G., Tanaka, K., Nakagawa, Y., Hoshi, M.: Study on Practical Conditions about Target Thickness and Gaussian Proton Energy using Near Threshold ${}^7\text{Li}(p,n){}^7\text{Be}$ Neutrons for BNCT. The Twelfth International Congress on Neutron Capture Therapy (ICNCT-12). Takamatsu, Kagawa, October 9-13, 2006.
26. 星 正治: 放射線と被曝についての解説. 第3回広島大学技術センター研修会. 広島, 平成18年11月27日.
27. 星 正治: 報告「これまでの被ばく線量研究とその役割」. ポストCOE第1回設立準備研究会「原爆・被ばく被害の包括的解明に向けて」(広島大学原爆放射線医科学研究所・文書館・平和科学研究センター共催). 広島, 平成18年12月19日.
28. Khvostunov, I. K., Nikjoo, H., Uehara, S., Hoshi, M., Endo, S.: The Microdosimetric Consideration of RBE of Low-Energy Proton on V79 Cells. III International symposium "Problems of Biochemistry, Radiation and Space Biology", Moscow, Dubna, January 24-28, 2007.
29. Endo, S.: First results of I-129 contamination in soil samples of Dolon village near Semipalatinsk Nuclear Test Site Area. 12th Hiroshima International -Symposium Radiation Effects in Semipalatinsk-. Hiroshima, March 2, 2007.
30. 星 正治: チェルノブイリやセミパラチンスクにおける放射線被ばくの調査研究. 平成18年度(第14回)救急医療研修会(福島県救急病院協会主催). 郡山, 平成19年3月8日.
31. 星 正治: 広島長崎の原爆線量評価システムDS02について. 筑波大学-KEK連携支援事業セミナー「マルチタンデム静電加速器による重イオンビーム学際利用への新展開」-UTTACの最新研究成果と動向-. つくば, 平成19年3月16日.
32. 星 正治: 放射線と被曝についての解説. 医療専門家による報告会〜ベラルーシでの医療支援活動をふり返って〜. 福岡, 平成19年3月18日.
33. Endo, S., Tomita, J., Tanaka, K., Yamamoto, M., Fukutani, S., Imanaka, T., Amano, H., Kawamura, H.,

- Kawamura, K. and Hoshi, M.: First results of ^{129}I contamination measurement in soil samples of the Dolon village near the Semipalatinsk Nuclear Test Site. 8th workshop for environmental radioactivity, Tsukuba, March 22-24, 2007.
34. 遠藤 暁：粒子識別型組織等価比例計数管(PID-TEPC)の開発. HIMAC共同利用研究成果発表会. 千葉, 平成19年4月9日-10日.
 35. 遠藤 暁：セミパラチンスク核実験場近郊土壌の ^{129}I 汚染量の測定－甲状腺線量推定法の開発として－. セッション4：放射線感受性や免疫影響の解析と影響評価に関する研究. 平成19年度特別教育研究経費. 第3回広島大学・長崎大学連携研究事業カンファレンス－国際放射線被ばく者先進医療開発研究の機関連携事業－. 広島, 平成19年6月2日.
 36. Hoshi, M.: Radiation dosimetry and its effects in Hiroshima and Nagasaki, Semipalatinsk and Chernobyl. International Conference “Peace Studies and Peace Discourse in Education”. Tomsk, Russia, June 14-16, 2007.
 37. Hoshi, M.: Dosimetry study for exposed people and its meanings. IPPNW 6th North Asia Regional Meeting, Ulaanbaatar, Mongolia, June 21-22, 2007.
 38. 星 正治：日米共同研究による広島・長崎の原爆放射線の見積もりおよびセミパラチンスク核実験場周辺住民の被ばくと健康影響. 九州大学, 福岡, 平成19年7月4日.
 39. 星 正治：集中講義. 放射線の被ばくとその影響の基礎について. 岡山理科大学, 岡山, 平成19年7月23日.
 40. 遠藤 暁：集中講義. 放射線の被ばくとその影響の基礎について. 岡山理科大学, 岡山, 平成19年7月24日.
 41. 遠藤 暁, 富田純平, 田中憲一, 山本政儀, 福谷 哲, 今中哲二, 天野 光, 川村秀久, 河村日佐男, 星 正治：旧ソ連核実験場近郊ドロン村から採取した土壌試料中 ^{129}I 汚染量の測定. 日本原子力学会中国・四国支部第1回研究発表会. 広島, 平成19年9月25日.
 42. 田中憲一, 遠藤 暁, 今中哲二, 葉佐井博巳, 星 正治：広島原爆の放射化土壌による β 線及び γ 線皮膚線量の評価. 日本原子力学会中国・四国支部第1回研究発表会. 広島, 平成19年9月25日.
 43. Hoshi, M.: Research standard in Japan. The Republican seminar - Master Class “The International research standards”. Semipalatinsk, Kazakhstan, September 27, 2007.

44. Hoshi, M.: System of research grants in Japan. The Republican seminar - Master Class "The International research standards". Semipalatinsk, Kazakhstan, September 27, 2007.
45. Hoshi, M.: Dosimetry Study for Exposed People and its Meanings. The 4th International Conference "Ecology, Radiation, Health". Semipalatinsk, Kazakhstan, September 28, 2007.
46. Hoshi, M.: Thyroid dose evaluation in Brest oblast, Belarus. Medical Symposium, Minsk, Belarus, October 23, 2007.
47. 遠藤 暁：霧箱で放射線・宇宙線を見てみよう。日本原子力学会オープンスクール。広島，平成19年11月3日。
48. 星 正治：原爆線量評価の変遷 物理学の観点から。放射線影響における「線量」を考える。日本放射線影響学会第50回大会。千葉，平成19年11月14日-17日。
49. 遠藤 暁，富田純平，田中憲一，山本政儀，福谷 哲，今中哲二，天野 光，川村秀久，河村日佐男，星 正治：旧ソ連核実験場近郊ドロン村から採取した土壌試料中¹²⁹I汚染量の測定。第50回日本放射線影響学会，千葉，平成19年11月14日-17日。
50. 田中憲一，遠藤 暁，今中哲二，葉佐井博巳，星 正治：広島原爆放射化土壌によるβ線及びγ線由来の皮膚線量の評価。第50回日本放射線影響学会。千葉，平成19年11月14日-17日。

研究成果

低エネルギー陽子線の照射による中性子の生物影響のメカニズム研究

星 正治

広島大学原爆放射線医科学研究所

間接電離粒子である中性子は、線量の90~95%を二次陽子が、残りの5~10%をその他の重イオン（酸素、炭素および窒素）が与えている。しかしながら、陽子線および重イオンのRBEは、2 ないし 3 であり、陽子と重イオンのRBEのLET依存性を用いて計算を行っても、中性子のRBE 7~10を陽子線および重イオンの重ね合わせで説明することはできない。線量は重ね合わせで説明できるにもかかわらず、その生物効果は全く説明できない。このことは、反跳核による線量測定、また生物効果の両方に対して未だ解明されていないことと関係がある可能性を示唆する。これまで行われている実験では、陽子線はサイクロトロン等の加速器からの数10MeV以上の陽子線照射がおもいで、高エネルギーの陽子線を用い、エネルギー吸収体を通して生物照射する。このため陽子線のトラック端での影響を見ている訳ではない。これに対し中性子線での実験では、線量は反跳陽子によって運ばれ、このエネルギーはまさに陽子線トラック端となっている。

中性子線の生物効果と陽子線の生物効果を比較検討するためには、陽子線トラック端となる中性子からの二次陽子のエネルギー領域で、RBEの陽子エネルギー依存性を見る必要がある。今回は理論的計算により、なぜそのRBEが大きいのか検討を加えた。

また中性子からの二次陽子のエネルギー領域における生物影響のデータはほとんど無く、このエネルギー領域で陽子線の生物影響を調べることは、中性子線の生物影響を考える上で重要である。我々は、この陽子線トラック端近傍で陽子線の照射を行う装置の製作を行い、実際に陽子線の大気取り出しを行った。中性子からの二次陽子のエネルギー領域で、RBEの陽子エネルギー依存性を見る必要がある。今回は筑波大学の2MV タンデトロン加速器からの陽子線を使用して、外装チェンバーとシリコンサーフェスバリアー型半導体検出器を使って細胞レベルでの線量測定の方法を検討した。

後半では、理論計算に基づいたそれぞれの細胞レベルでの陽子線照射を行った際にそのRBEがどのように変化するかの計算結果とその考察を示す。

(1) イオンチェンバーを使った細胞内線量評価の検討

星 正治、遠藤 暁

広島大学原爆放射線医科学研究所

はじめに

先に述べたとおり、陽子線のトラックの終端のエネルギー領域で陽子線の生物影響を調べることは、中性子線の生物影響を考える上で重要である。その際の線量評価をどう測定してどう評価するかについてはまだ明確な方法は確立していない今回は筑波大学の2MV タンデトロン加速器からの陽子線を使用して、外装チェンバーとシリコンサーフェスバリアー型半導体検出器を使って細胞レベルでの線量測定の方法を検討した。

目的

本研究グループでは、広島・長崎の被ばく線量の評価を行ってきた。その被ばくには中性子の影響も含まれるが現在では中性子線量がガンマ線量に対して少なく、その影響の程度は分かっていない。

中性子の被曝の特徴は、中性子自身でなく、2次的に発生する荷電粒子によってのみ生物に影響を与えることである。その影響の大きさ (RBE) は、ガンマ線やX線と比べて2~3倍の場合もあるが、7~10倍やさらにそれより大きい場合も多い。その2次的電離粒子のうち、線量の70%-80%を反跳陽子が、残りの20-30%をその他の反跳核 (ヘリウム、酸素、炭素および窒素など) が与えている。しかしながら、陽子線および他の反跳核のRBEは、大きくても2ないし3であり、陽子と他のイオンのRBEのLET依存性を用いて計算を行っても、中性子のRBEが7-10にもなることを説明することは容易でない。

本研究では、この理由について考察することを目的とする。最終的には、細胞に対して陽子線の照射をし、その影響を調べる。細胞照射は膜の上に1層付着した状態で行う。細胞は数ミクロン程度の厚さである。エネルギーが高ければ細胞を通過し線量の評価は可能である。今まで、より高いエネルギーの実験は存在するが、エネルギーの低い、ブラッグピーク近傍やさらに低い止まり際の線量評価は容易でなく、行われていない。この実験を行うためには、実験システムや線量評価法を含めた検討が必要である。

平行平板でその厚さを変えることができる、外挿チェンバーを使って空気中のイオン化を測定し線量进行评估する方法を確立する。

実験概要

大気取り出し陽子線の線量測定は、筑波大学加速器センター 2 MeV タンデトロン加速器を用いた。タンデトロンで 1.92 MeV に加速した陽子線を 2.5 μm ハーパーフォイル窓 (直径 1 cm ϕ) を通して大気中に取り出した。大気取り出し陽子線のフラックスをモニターするため、大気取り出しチャンバー中に金 1 μm または炭素薄膜 32.1 $\mu\text{g}/\text{cm}^2$ のラディエータを設置して、ラディエータにおけるラザフォード散乱される陽子を測定し陽子線 flux のモニターに用いた。図 1 にビームモニターに用いたラザフォード散乱陽子線のスペクトル例を示す。

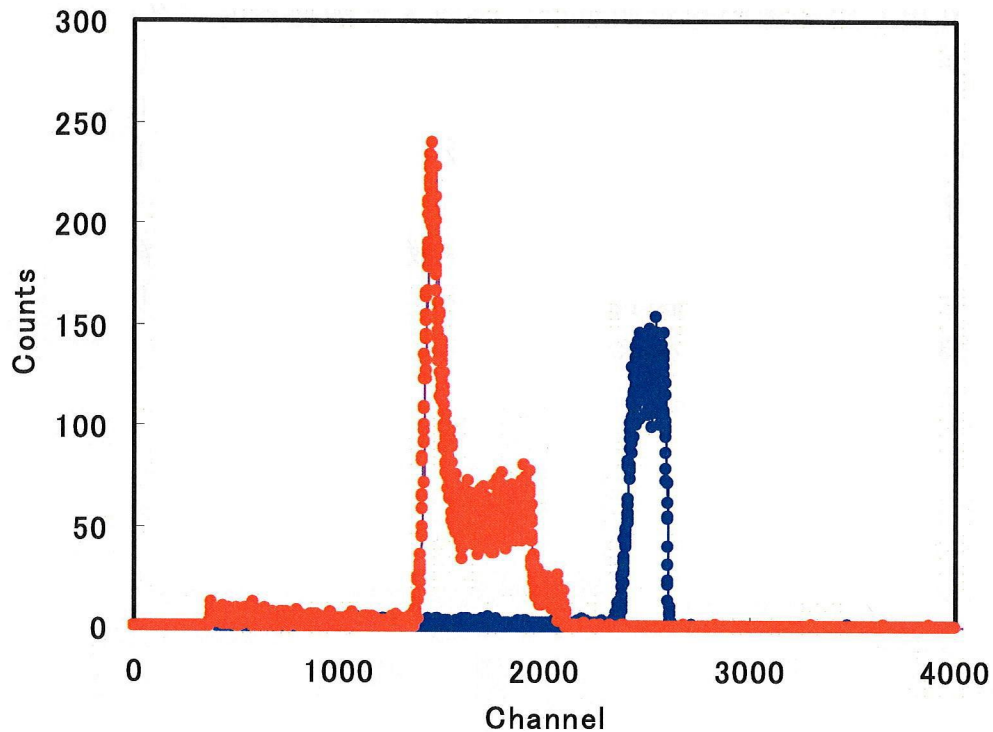


図1：ビームモニターに用いたラザフォード散乱陽子線のスペクトル。

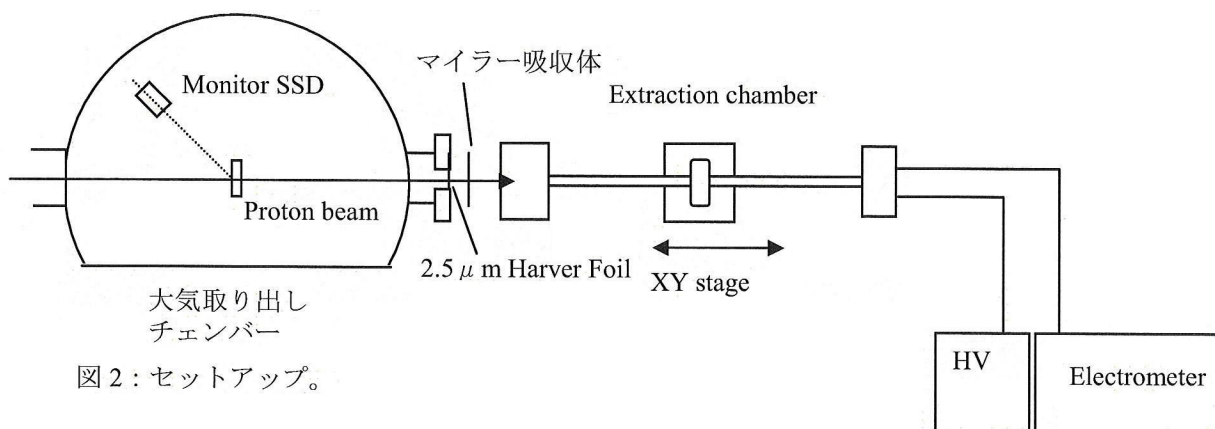


図2：セットアップ。

線量測定には外挿チェンバー(Farwest Technology inc. EIC-1)を用いた。外挿チェンバーは、入射窓およそ $2\mu\text{m}$ の極薄の窓で、直径 $10\text{mm}\phi$ の円筒の厚さを任意に変えることの出来る特殊な電離箱である。セットアップを図2に示す。大気取り出しビームの細胞などの生物試料への照射線量を評価するため、大気取り出し窓と外挿チェンバーの間にマイラーを挿入し、線量のマイラー厚さ依存性を測定した。更に、各マイラー厚さ

時のエネルギースペクトルを確認するため表面障壁型Si検出器を外挿チェンバーと交換して測定を行った。

結果

外挿チェンバーによる測定結果を図3に、表面障壁型Si検出器による測定結果を図4に示す。マイラー厚さを増やすと共に、徐々に線量は上昇し、21-25 μm で最大値となり、更に厚くすると減少する。これは、荷電粒子のブラッグピークの傾向に一致している。これに対し表面障壁型Si検出器の場合では、空乏層内で全エネルギーを吸収するためブラッグピークは表れず、飛程が確認できる。

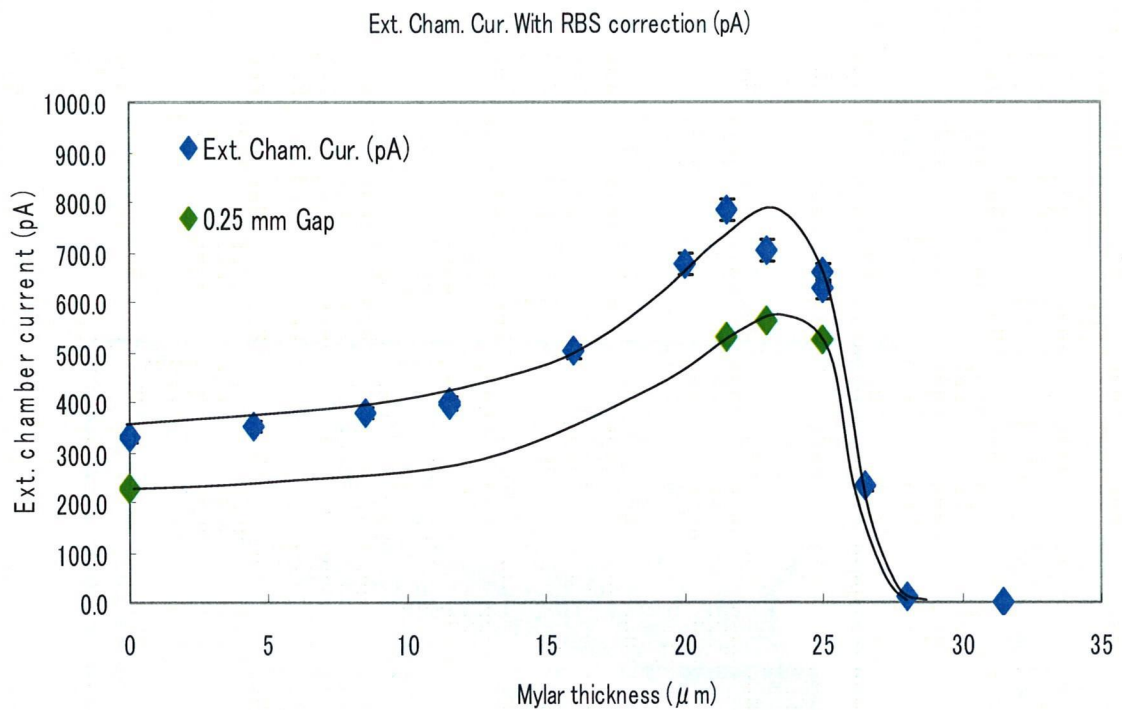


図3：外挿チェンバー電離量のマイラー吸収体厚依存性。

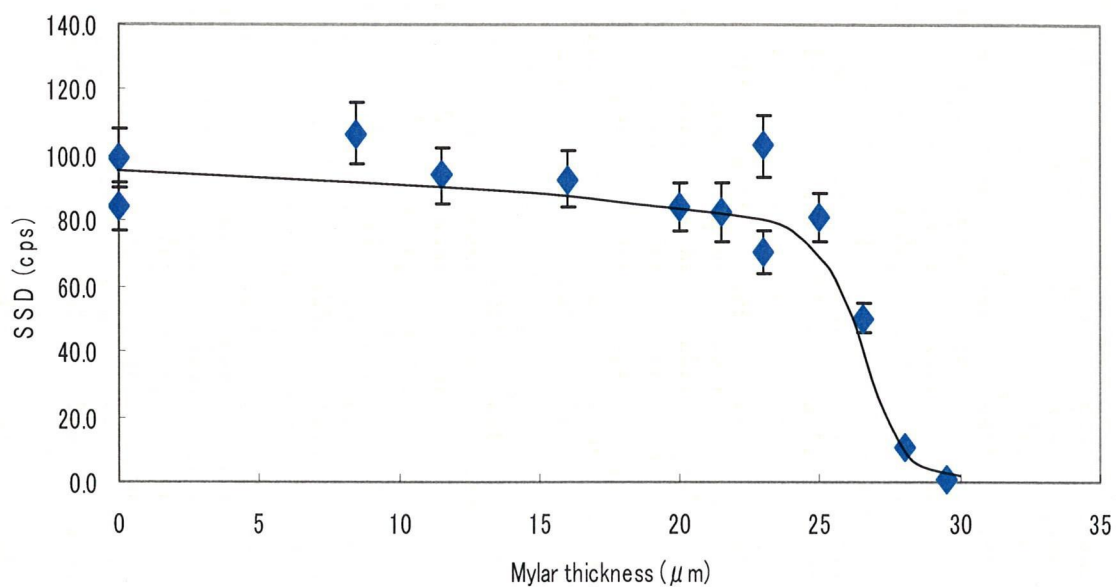


図 4 : 表面障壁型 Si 検出器カウンティングレイトのマイラー吸収体厚依存性。

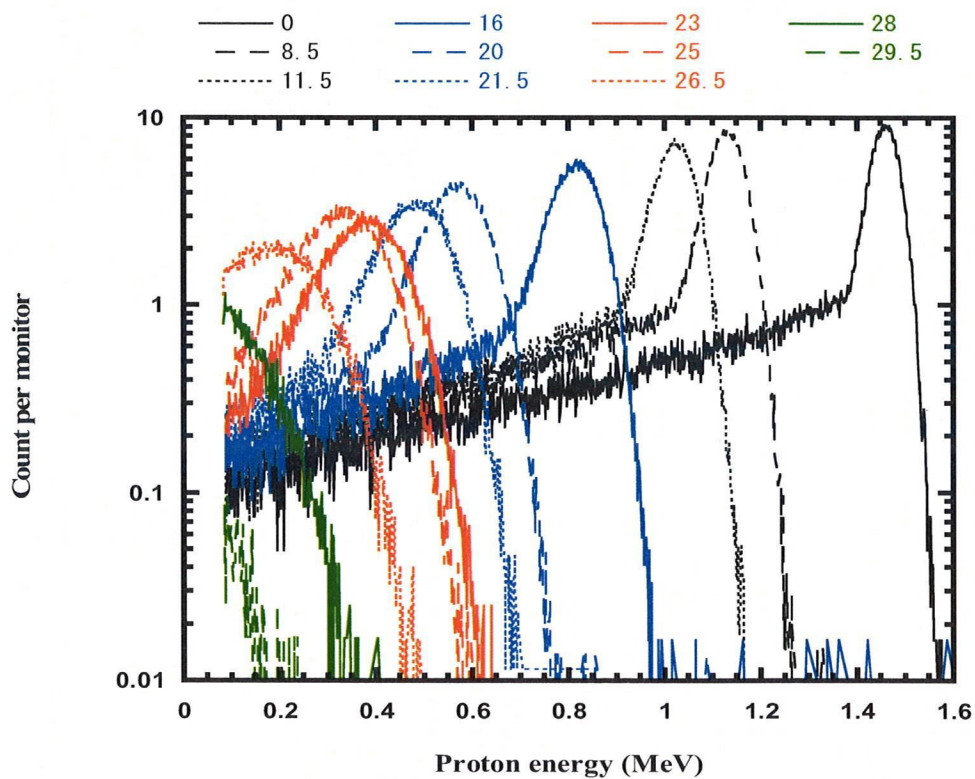


図 5 : 表面障壁型 Si 検出器を用いた大気取り出しビームのエネルギースペクトル。

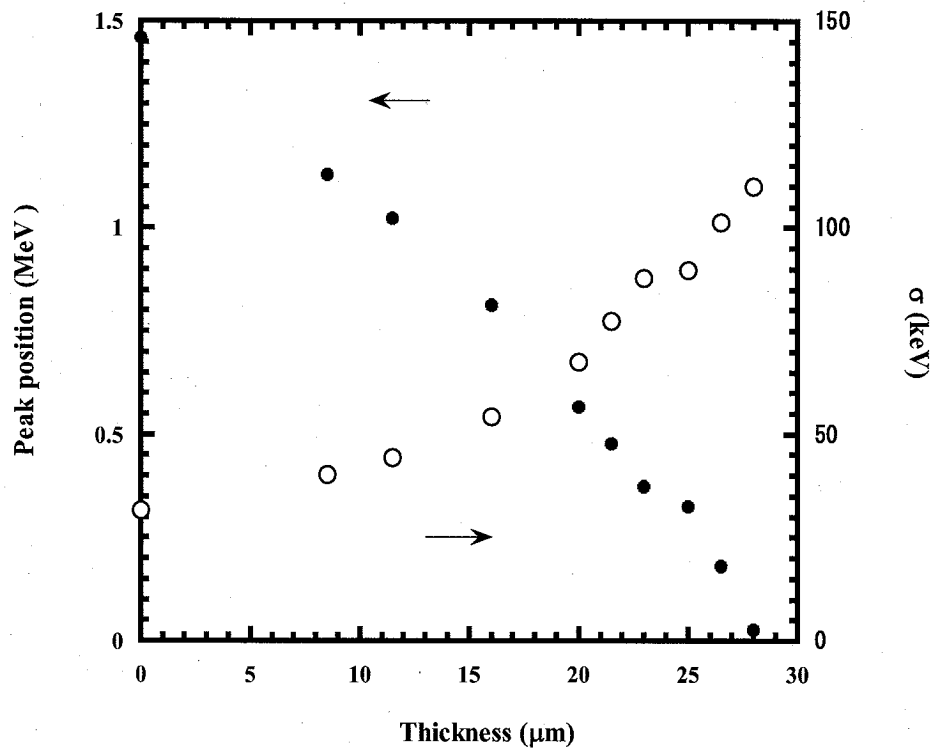


図6：図5に示したスペクトルの各 peak position と peak sigama。

各マイラー吸収体厚みでの表面障壁型Si検出器の測定スペクトルを図5に示す。吸収体で付与したエネルギー分だけエネルギーが低くなることに加え、エネルギー広がりが増加することが確認できる。各スペクトルをガウス分布で近似した場合のピーク位置とエネルギー広がりを図6に示す。測定に利用したSi検出器の $^{241}\text{Am}-\alpha$ 線に対する分解能は28keVであるので実際の陽子エネルギーの広がりには10keV-106keVと予想される。

ビームプロファイル

大気取り出し後の陽子線のプロファイルを確認するためZnSシートを取り出し窓に貼付け確認した。写真を図7に示す。陽子線は取り出し窓いっぱい広がっていることが確認された。またビームは比較的一様に広がっており、生物実験には適したビームであった。

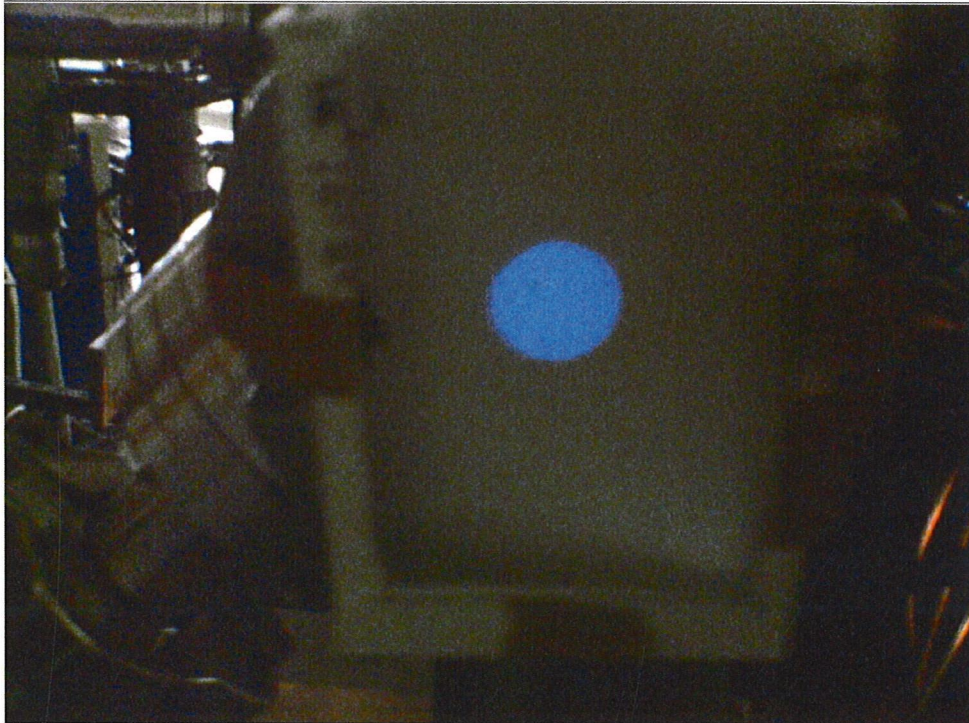


図7 : ZnS によるビームプロファイルの確認。

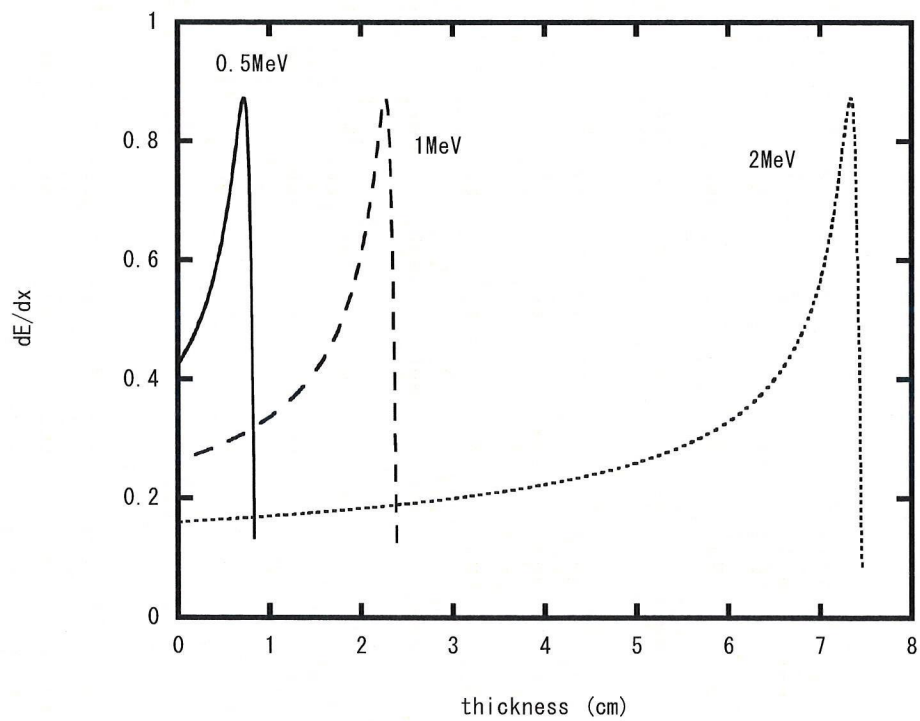


図8 空気吸収体厚さに対する陽子線のブラッグピーク計算値

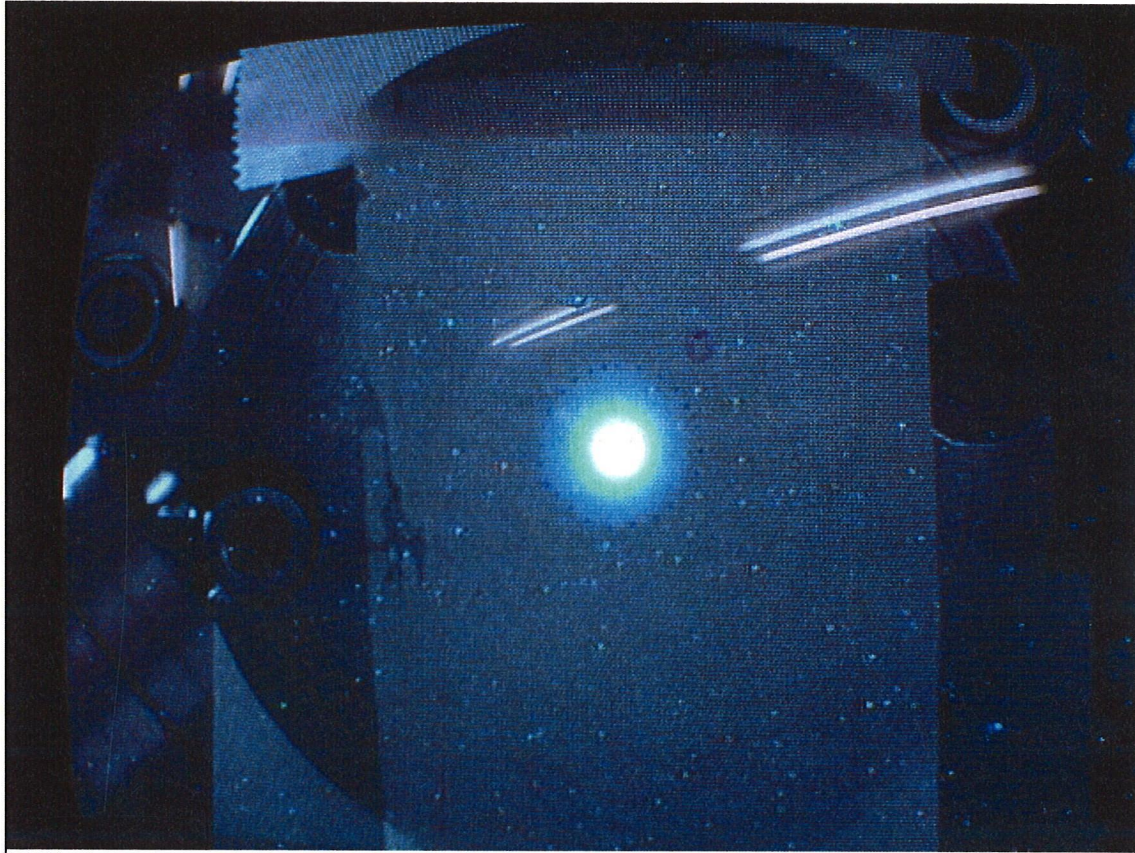


図9 ナロービーム条件のビームプロファイル

ナロービームでの確認

図5に示すように、本測定において確認されたブラッグピークはピークプラトー比が2:1程度であり、計算上で得られる値、およそ4:1と比較するとかなり小さい。参考として0.5MeV、1MeVおよび2MeVに対する計算を図8に示す。この原因としてビームモニター用散乱体、大気取出し窓端、またマイラーなどによる散乱陽子による効果の可能性がある。確認のため、ビームモニター用散乱体厚を出来る限り薄くし(32.1 $\mu\text{g}/\text{cm}^2$)、ナロービームを用いて空気中での外挿電離箱測定を行った。ナロービームのプロファイルを図9に示す。破線が大気取出し窓を示す。したがって、主たるビームは窓端には当たっていないことが確認できる。

外挿電離箱の測定結果を図10(a)、(b)に示す。(a)は電離箱の有感厚を1mmと2mmに設定した測定であり、(b)はこの測定値の差をとったものである。外挿チャンバーを用いた線量測定では、有感領域の体積を変化させ差を取ることで入射窓等の効果を差引く手法が用いられる。本測定においては、有感領域の厚さを1mmから2mmにした際の差の部分が本来の

線量を示すことになる。2mm厚と1mm厚で電離電荷の差を示す図10(b)では、ピークプラトー比は3.2:1であり、計算値の4:1に近づく。この値に、W値のエネルギー依存性(図11参照)を考慮すると、3.7:1でほぼ計算値に一致する。これらのことより、測定法自体の問題はなく、実際に図5の照射条件では、吸収体のマイラー厚さに依存したブラッグピークがえられていると考えると差し支えない。

線量評価

外挿チェンバーの電離電流は、原医研⁶⁰Co γ 線照射装置が現在使用不能のため校正が出来ず線量絶対値に変換することが出来ない。そこで、SSDの波高分布よりおおよその値を評価した。粒子当たりの線量は dE/dx より特徴付けられるため、 dE/dx の平均値をスペクトルより以下の式で求めた。

$$\overline{(dE/dx)} = \frac{\sum_{i=0}^N f(E_i) \cdot dE/dx(E_i)}{\sum_{i=0}^N f(E_i)}$$

また、エネルギー付与から線量进行评估するため、以下の定数を用いる。

$$\begin{aligned} 1\text{keV}/\mu\text{m} &= 1 \times 10^3 (\text{eV}) \times 1.602 \times 10^{-19} (\text{C}) / \{10^{-4} (\text{g}) \times 10^{-3} (\text{kg/g})\} \\ &= 1.602 (\text{nGy}) \end{aligned}$$

この値を利用すると、マイラーなしの状態で36.2nGy/p、また最大になるのはブラッグピーク上で(今回の測定ではマイラー厚25 μ m)、49.5nGy/pと考えられる。この値より 2×10^7 pでおおよそ1Gyであり、陽子電流3.2pAで運転し、1Gy/sの線量率と考えられる。

まとめ

大気取出し陽子線を用いた実験システムと線量評価法を含めた検討を行い、基本的な方法を決定した。原医研⁶⁰Co γ 線照射装置が使用できなかったためにSSDスペクトルを用いて線量进行评估したところ、吸収体無しで36.2nGy/p、ブラッグピークの上で49.5nGy/pの値が得られた。この値を電離箱データを用いて確認することが必要である。今後、生物照

射実験を行っていく。

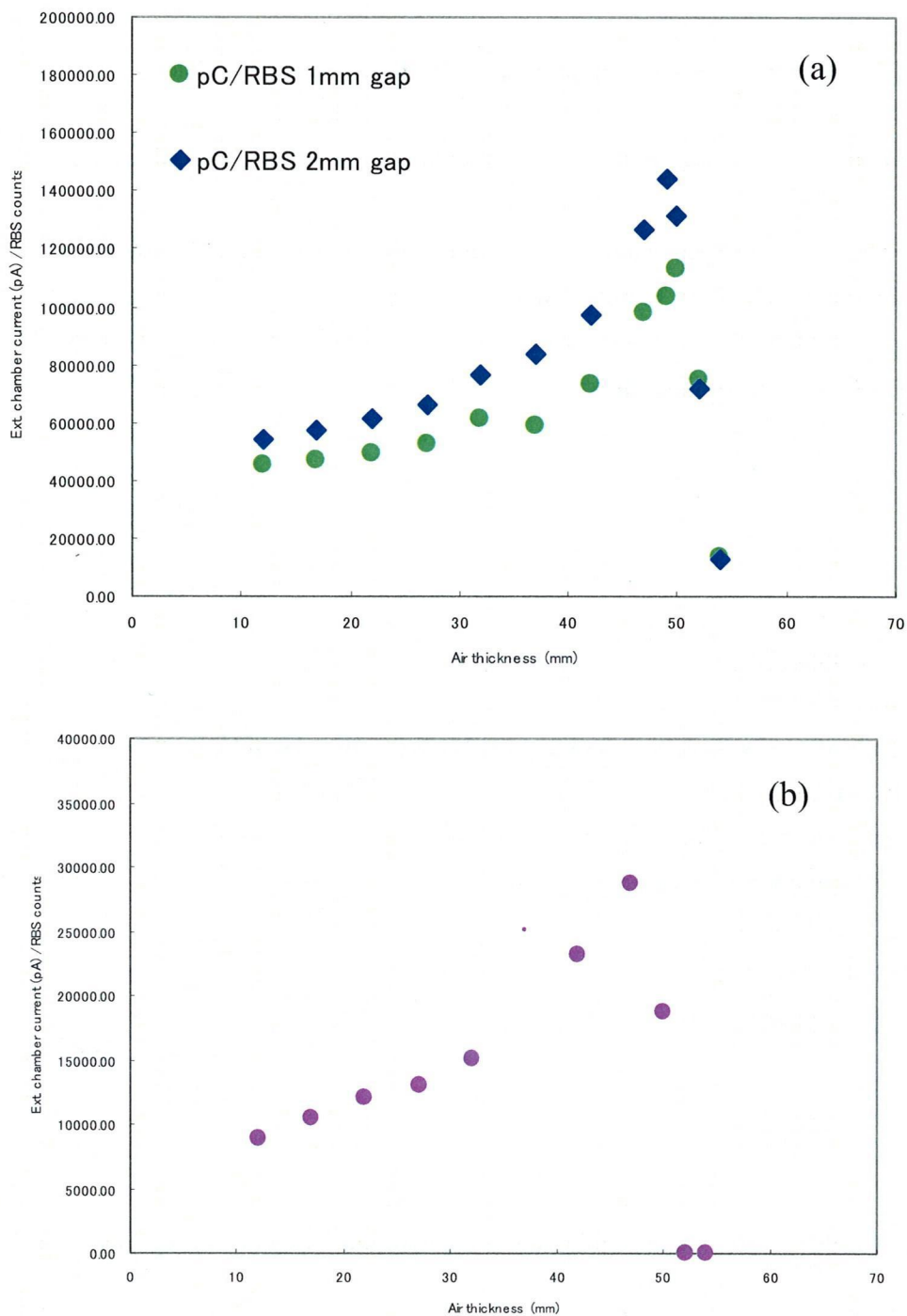


図 10 (a)外挿チェンバーの有感領域の厚さ 1mm と 2mm に設定した場合の空気吸収体厚の電離量依存性。(b)有感領域の厚さ 2mm-1mm の電離量。

(2) The consideration of biological effectiveness of low energy protons using biophysical modeling of exposure of V79 cells

Igor K. Khvostunov¹, Hooshang Nikjoo², Shuzo Uehara³, Masaharu Hoshi⁴

¹Medical Radiological Research Centre, Koroliov St. 4, Obninsk, Kaluga Region, 249036, Russia

²Center for Advanced Space Studies, NASA Johnson Space Center, Houston, USA

³School of Health Sciences, Kyushu University, Japan

⁴Research Institute for Radiation Biology and Medicine, Hiroshima University, Minami-ku, Kasumi, 734-8553 Hiroshima, Japan

Author for correspondence:

Masaharu Hoshi, Ph.D.

Research Institute for Radiation Biology and Medicine Hiroshima University

1-2-3 Kasumi, Minami-ku

Hiroshima 734-8553

e-mail: mhoshi@hiroshima-u.ac.jp

TEL: +81-82-257-5872,

FAX: +81-82-257-5873

mhoshi@hiroshima-u.ac.jp

Indexing terms: RBE, Monte Carlo, low energy protons, microdosimetry, DNA damage

Abstract

We have applied the stochastic track structure technique for the biophysical simulation an irradiation of growing in mono-layers V79 cells with low-energy protons. It was studied the microscopic energy deposition in cell nuclear and sub-nuclear volumes to get better understanding the peculiarities of low-energy proton irradiation resulted in enhanced biological effectiveness near Bragg peak. It was followed the possible correlation between experimental estimation of RBE_M and theoretical values: frequency/dose averaged linear energy and calculated yield of initial complex DSB breaks. It was found: (i) dose averaged, y_D , values for whole cell nuclear as a function of proton energy has a single peak at 550 keV; (ii) the peak value is sufficiently larger for local sub-nuclear sensitive volumes than for whole cell nuclear (iii) in the spectrum of initial DNA breaks only complex breaks can correlate with experimental data on RBE_M .

Introduction

The study of relative biological effectiveness (RBE) of low-energy protons and neutrons attracts considerable interest for many scientific fields: conventional radiobiology, radiation protection, radiation risk estimation etc. ¹⁻³⁾. At that an understanding the role of low energy protons solely is the basic point to elucidate specific mechanisms of such radiation action ⁴⁾. Basically the values of RBE are derived from radiobiological data defining as a ratio of reference dose to the dose of tested radiation to produce the same biological effect. For the purposes of radiation protection the main field of interest is a RBE values at low doses, when dose response function is linear and RBE tends to the quotient initial slopes denoted as RBE_M . It is believed this value is the maximal RBE at low doses.

The intrinsic reason of expected increasing the RBE_M values of protons in the energy range characteristic of the Bragg peak is still the matter of scientific discussion. Therein this study of microscopic energy deposition in cell-subnuclear targets is the further step toward better understanding the peculiarities of low-energy proton irradiation resulted in enhanced RBE near Bragg peak. The used microdosimetry approach is rather universal and mathematically applicable for theoretical estimation both RBE values and average quality factor $\langle Q \rangle$ ⁵⁾.

In experiments the variation of RBE_M with proton or neutron energy has been investigated using mainly cellular data on survival and mutation assays as well as chromosomal aberrations ⁶⁻⁷⁾. Herewith an observed particular RBE_M values are depended on object, endpoint, radiation field and reference radiation. As a result there are a plenty of experimental data, sometimes differ each other in the values of RBE_M . For better understanding, correct interpretation of radiobiological data and more realistic rather conservative approach for determination a quality factor the analysis of data should be supplied by biophysical computer modeling.

Our purpose was to present theoretical results on microdosimetry modeling exposure of V79 cells using stochastic track structure of low energy protons up to full slowing down. Besides, it was calculated the spectra of initial DNA breaks according to its complexity to test the hypothesis ⁸⁻¹⁰⁾ whether a complex double strand breaks (DSB) could sometimes correlate with observed variation of RBE_M . In this paper an irradiation of V79 cells growing in mono-layers and exposed with low-energy protons was simulated. The stochastic effects of exposure were investigated by modeling the pattern of energy deposition in cell nuclear and sub-nuclear volumes. It was followed the possible correlation between experimental estimation of RBE_M and theoretical values: frequency/dose averaged linear energy and calculated yield of initial complex DSB breaks. The presented quantitative modeling is expected to be useful tool for interpretation of observed RBE_M values derived from cell inactivation and mutation data as a function of initial energy of protons.

Methods

Proton tracks

The details of stochastic track structure simulation, estimation of microdosimetry spectra and DNA breaks induction have been published previously ¹¹⁻¹²⁾. In brief, proton tracks with incident energy in the range 1 keV – 1 MeV were generated by the *LepHist* code ¹¹⁾, and proton track segments with energy in the range 1 MeV – 10 MeV were generated by *Pits* code ¹³⁾ in liquid water of unit density. All primary interactions, including elastic scattering, ionizations, excitations and charge exchange processes by protons and neutral hydrogen were taken into account. The primary protons generated by *LepHist* were followed from initial energy down to 1 keV. Secondary electrons produced by ionizations were followed down to energies below 1 eV then assumed to be locally absorbed. Both in *LepHist* and *Pits* code the same routine *Kurbuc* ¹⁴⁾ were used for generation secondary electron tracks. The codes have been analyzed to provide the reliability on physical quantities such as full range, W-value, stopping power and radial dose profiles showing good agreement with experimental and theoretical data ¹⁵⁾.

Biological target

In line with analyzed experimental data the following geometry of thin mono-layer has been considered ¹⁶⁻²⁰⁾, see fig.1. In those experiments V79 cells are usually grown attached on mylar surface and the low energy proton beam goes sequent through mylar base, cell membrane, cytoplasm and cell nuclear as shown in fig.1. It was shown by fluorescence microscope measurements ²¹⁾ that the shape of V79 cell nucleus is similar to a rotation ellipsoid of 15 μm wide and 8 μm high. The value used in this paper for cytoplasm thickness between base and nucleus was assumed to be 1 μm base ²²⁾. The variation of target size parameters due to non-homogeneous cell population was not considered in this study.

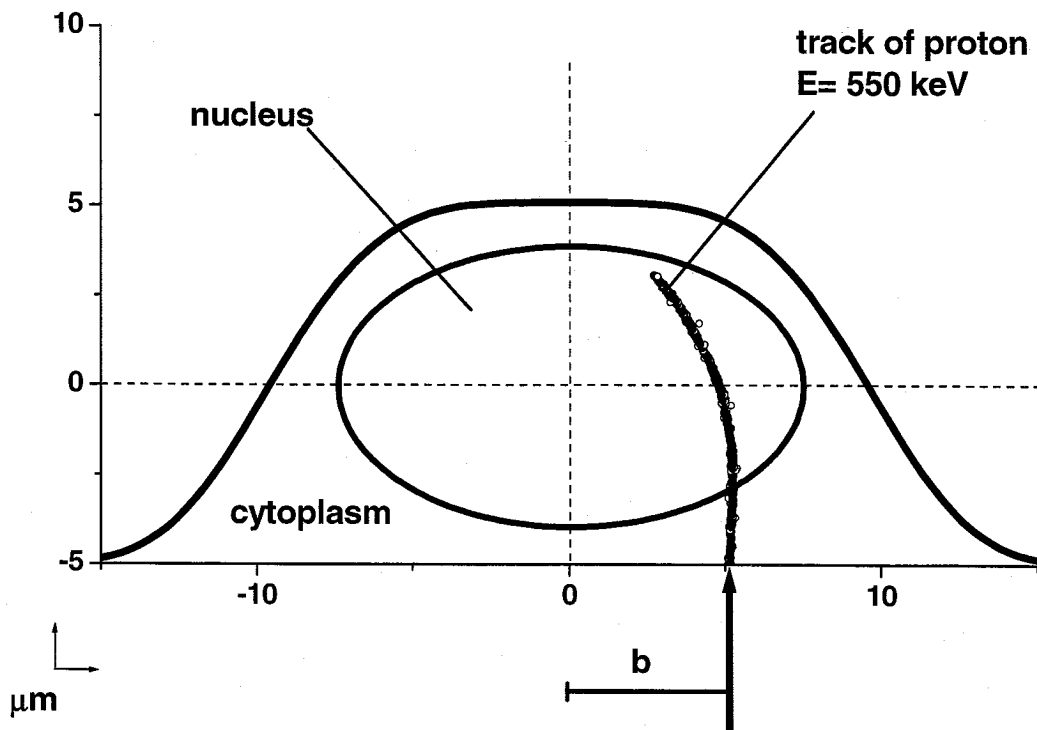


fig. 1 The schematic shape of cytoplasm and nuclear in a V79 cell used in the simulation of mono-layer experiments with irradiation cells by protons. b – impact parameter.

Simulated irradiation conditions

The irradiation of V79 cell monolayer with parallel proton beam incident along Z-axis was considered using microdosimetry approach ²³⁾. First, it was calculated microdosimetry frequency distribution, $f(y)$, of linear energy, $y=\varepsilon/\langle l \rangle$, where ε - energy imparted in the target volume, $\langle l \rangle$ - mean chord length. For this case the superposition of single proton track located at given impact parameter, b , see fig.1 and target volume was tested repeatedly. The homogeneous distribution on base surface for 'b' was used and linear energies were scored to estimate statistically a frequency averaged, y_F , dose averaged, y_D , values and corresponded distributions ²³⁾. Those values are defined as follows

$$y_F = \int y f(y) dy; \quad y_D = \int y d(y) dy, \quad \text{where} \quad d(y) = \frac{y f(y)}{y_F}$$

Second, the irradiation to proton beam at given dose D was simulated as following. The

mean number $\langle N \rangle$ of proton traversals per target area, S , was calculated as $\langle N \rangle = 6.2 \cdot D \cdot S / \text{LET}$, where D in Gy, S in μm^2 , and LET in $\text{keV}/\mu\text{m}$. For the elementary simulation the actual number of traversals was extracted from Poisson distribution with expected averaged value $\langle N \rangle$. This type of simulated irradiation was used for estimation the efficiency of DNA breaks per Gy as a function of absorbed dose according to experimental conditions of V79 cells exposure.

Biophysical estimation

In calculations of microdosimetry spectra the following types of targets were considered. The first case we consider the whole cell nucleus generated by the rotation of the ellipsoid shown in fig. 1. In the second case, the absorbed energy was scored in a spherical volume with diameter $1 \mu\text{m}$ (ICRU sphere)⁵⁾ located along the short axis of cell nucleus. In the case of parallel beam, the mean chord length in a spherical volume equals to $2 \cdot d/3$, where 'd' is the diameter of sphere. But for the case, where the target is generated by the rotation of ellipsoid of the same mass and unit density irradiated along its short axis the mean chord length is $2 \cdot e/3$, where 'e' is the short axis of ellipsoid which is less than sphere diameter. However, in the case when full range of proton track is much larger compared with the pathway in the target, the distribution and mean lineal energy in a sphere and rotation ellipsoid tend to be approximately similar. In general, the spectra for the two geometries differ owing to larger energy loss in a sphere.

In addition, we calculated the yield of DNA damage. For this purpose we used a linear section of DNA of 300 nucleotide pairs randomly orientated with respect to proton beam direction. The canonical linear double stranded B-DNA was applied for twin helix. The volume model of DNA and model of strand breakage have previously been described in details¹²⁾. It has been assumed that energy deposition of 17.5 eV or more in sugar-phosphate moiety results in induction of a SSB. Two SSB on opposite strands less than 10 base pairs (bp) apart were scored as one DSB. The yields of SSB and DSB were further classified by complexity¹²⁾.

Results

The calculated contributions of given linear energy in an absorbed dose in V79 cell nuclear are presented in fig 2. It was plotted the following functions: $y f(y)$ and $y d(y)$, see "Methods", so the areas under the curves equal to frequency mean, y_F (panel A) and dose averaged, y_D , (panel B) values respectively. As it is defined in microdosimetry²³⁾ such spectra show the compound of frequency averaged value y_F , which is microdosimetry analogue of LET, and dose

averaged value y_D , that relates to absorbed dose. Thus, it can prompt what particular range of linear energy (or LET) is mainly responsible for the observed effect in irradiated V79 cells⁵⁾.

Depending of impact parameter 'b' the path-length of proton in a cell nuclear varies from 0 to 8 μm with the average chord equals to 5.3 μm , see fig. 1. So, a 10 MeV proton (LET=4.5 keV/ μm) losses very small part of initial energy in cell nuclear. The dispersion of linear energy shown in fig 2 is basically due to geometry fluctuations of path-length and dispersion of energy loss. The contrary case is for the 550 keV (LET= 39 keV/ μm) protons. They enter the cell nuclear with the energy about 510 keV (LET= 40 keV/ μm) get over 1 μm path in cytoplasm, so the entering energy is a little bit less than energy of proton incident on a cell. The range of 510 keV protons is comparable with cell nuclear size, so they can fully absorb in the target. In this case the linear energy ranges up to $(510/5.3)=96$ keV/ μm resulting from full slowing down of proton inside the cell nuclear. Besides, it can be seen that linear energy distributions of 550 keV protons are significantly asymmetrical, pointing out that events with linear energies much higher than LET of initial proton assume to be the most important for the expected radiation effect.

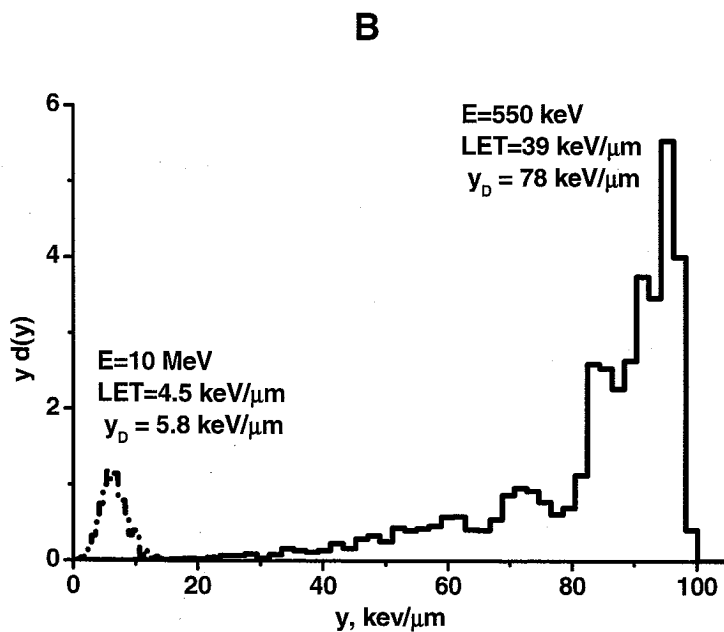
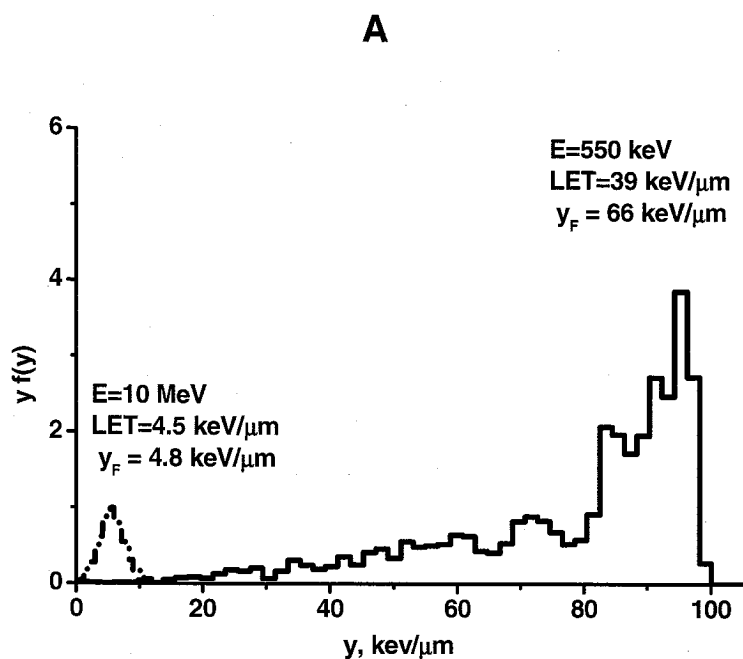


Fig. 2 Calculated linear energy distributions of 10 MeV and 550 keV protons in a cell nuclear. Shown are the $y f(y)$ (panel A) and $y d(y)$, (panel B), so the areas under curves equal to frequency, y_F , and -dose averaged, y_D , values respectively. The structures in the curves are of statistical nature.

In the fig. 3 the calculated y_F , and y_D , values using whole cell nuclear are shown as a function of initial energy of proton entering a V79 cell. The dotted line is LET of those protons²⁴⁾, added in the plot for comparison. It should be noted that low-energy protons with energy less than 70 keV, are not able to give rise a non-zero energy deposition in a cell nuclear due to its short range, less than thickness of cytoplasm between base and nucleus (about 1 μm , fig.1). The above energy threshold is a little bit higher 50 keV, for which range of proton equals to 1 μm ²⁴⁾. The reason is significant space curvature of proton tracks full slowing down in cytoplasm, so only protons with energy 70 keV or more can reach a cell nuclear after crossing 1 μm of cytoplasm. Then it can be seen from fig 3 the calculated values are plotted from 70 keV to 10 MeV showing the clear peak at 550 keV. At that comparing the range of protons entering cell nuclear (510 keV, range is about 9 μm) with maximal nuclear size (8 μm) it can conclude that the maximum of mean linear energy is expected when residual range of entering protons exceeds the size of target by about 10-12%.

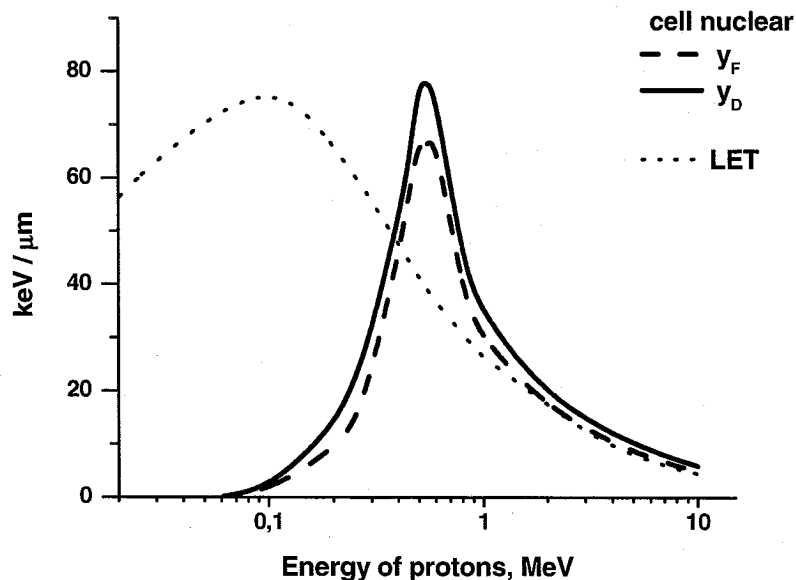


Fig. 3 Calculated frequency averaged, y_F , and dose averaged, y_D , values using a cell nuclear as a function of initial proton energy. The solid line represents LET of protons²¹⁾ shown for comparison.

An expected non-homogeneous distribution of imparted energy in a V79 cell nuclear was examined in the following way. It was tested the two limiting locations in a nuclear: at a top and at a bottom of nuclear. For this a ICRU microdosimetry sphere (1 μm diameter)⁵⁾ was used as a sensitive virtual detector. The following two limiting locations of this sphere in a cell nuclear were tested: (1) – at the bottom of cell nuclear, i.e. at the nearest point to a proton beam enter

and (2) at the top of cell nuclear axis – the most distant from proton beam, see fig.1. The calculated frequency averaged, y_F , and dose averaged, y_D , values using ICRU sphere are shown in the fig. 4 as a function of initial proton energy. In the case (1) proton passes the way at least $1 \mu\text{m}$ to enter the sensitive volume whereas in the case (2) such a way is about $8 \mu\text{m}$. So, in the case (2) the curve is drawn from 460 keV (protons of this energy have a range about $8 \mu\text{m}$) to 10 MeV. Then it can be seen from fig 4 the calculated linear energies show the peaks at 250 and 600 keV for the locations (1) and (2) respectively. Depending on the rest of possible locations of ICRU sphere along cell nuclear axis the corresponding peaks of mean linear energy are expected to range from 250 to 600 keV of initial proton energy.

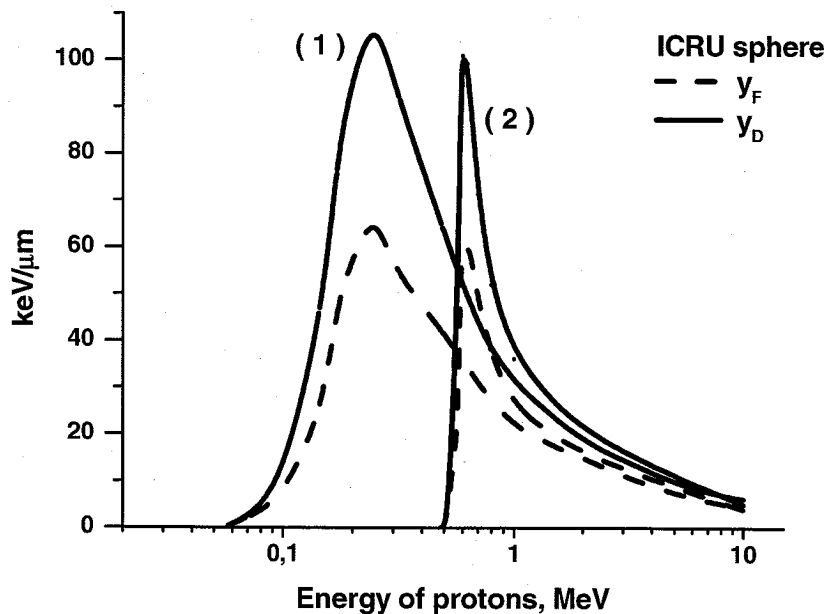


Fig. 4 Calculated frequency averaged, y_F , and dose averaged, y_D , values using a ICRU sphere ($1 \mu\text{m}$ diameter) located in a cell nuclear at the nearest (1) and the most distant (2) points from proton beam entry.

The calculated linear energy distributions of 250 keV and 10 MeV protons in ICRU sphere located in a cell nuclear at the nearest point to proton beam entry (1) are shown in the fig 5. Compared with the whole cell nuclear a linear energy in ICRU sphere is distributed rather broadly, up to $160 \text{ keV}/\mu\text{m}$. Such linear energy is the result of energy deposition of 107 keV that is more than half of proton energy entering a cell. Indeed, 250 keV proton ($\text{LET}=61 \text{ keV}/\mu\text{m}$) passes $1 \mu\text{m}$ of cytoplasm before it enters to the target. Besides, in the contrast with whole cell nuclear case, for ICRU sphere the y_F value is about twice less y_D . Such a difference is a reliable sign of increasing the role of microdosimetry fluctuations of linear energy with

decreasing the size of a target. It is a well-known condition for needless of microdosimetry approach ²³⁾ instead of usual dosimetry.

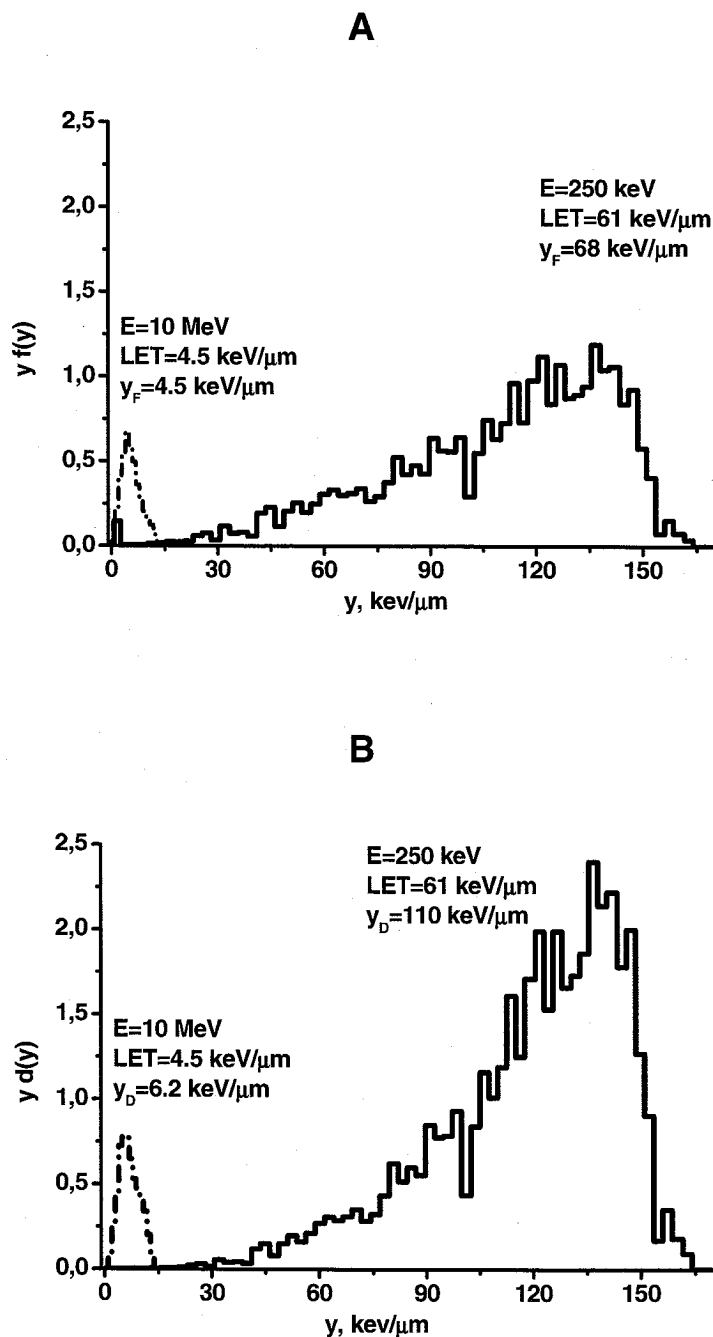


Fig. 5 Calculated linear energy distributions of 10 MeV and 250 keV protons in a ICRU sphere ($1 \mu\text{m}$ diameter) located in a cell nuclear at the nearest point from proton beam entry. Shown are the $y f(y)$ (panel a) and $y d(y)$, (panel b), so the areas under curves equal to frequency, y_F , and -dose averaged, y_D , values respectively. The structures in the curves are of statistical nature.

In the fig. 6 the calculated dose averaged, y_D , linear energy using three different sensitive volumes are shown as a functions of initial energy of proton entering a cell. It was considered whole cell nuclear calculations compared with ICRU sphere located in a cell nuclear at the nearest and the most distant point from proton beam entry: (i) – at the bottom of cell nuclear, i.e. nearest to proton beam enter and (ii) at the top of cell nuclear axis – the most distant from proton beam, see fig.1. The curves of whole nuclear and ICRU sphere (i) are plotted on the same range of proton energy from 70 keV to 10 MeV but show the different location of peaks and heights at the peak. The y_D drop between 10 MeV and peak value is 13 for cell nuclear curve and 18 for ICRU sphere (i). The curve of ICRU sphere (ii) shows about the same drop as (i) but is shifted towards higher proton energies. The other possible locations of ICRU sphere in a cell nuclear distributed between two limit points (i) and (ii) are expected to show the curves with the similar drop at maximum as presented in fig. 6 and distributed between curves (i) and (ii).

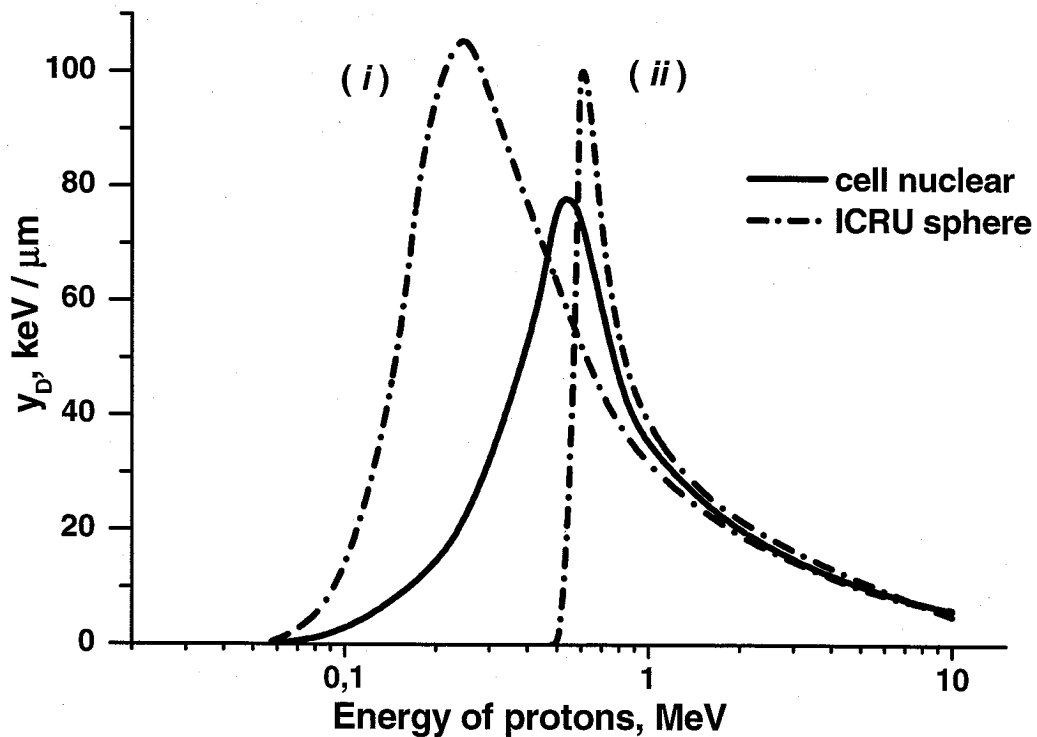


Fig. 6 Calculated dose averaged, y_D , values using a cell nuclear and ICRU sphere located in a cell nuclear at the nearest (i) and the most distant (ii) point from proton beam entry.

It was pointed out that cellular effects of ionizing radiation could be determined by ionization clusters at the level of DNA molecule, rather than at the level of micrometers sensitive volumes⁸⁻¹⁰). Therefore the quantitative modeling of initial DNA damage in the segment of DNA was carried out to test the various types of strand break which do or do not correlate with observed biological effectiveness as a function of initial proton energy. To investigate this statement, first, it was calculated the yields of DNA breaks using virtual geometry when protons expose segment of DNA straightforwardly with no slowing down way before this target. In this case the yields of DNA breaks can be estimated from the lowest energy of protons, about couple of keVs.

In the fig.7 the yields of DNA breaks per Gray per Dalton simulated in short DNA segment are shown as a function of initial energy of proton affected straightforwardly to the DNA. Those results were calculated to show the shape of DNA breaks as a function of proton energy when protons directly affect DNA. So that, the proton energy ranges from about 5 keV to 10 MeV. Panel A of fig. 7 presents SSB and panel B - DSB according to their complexity. The results are presented for simple and complex strand breaks separately for three types of single breaks (ssb, ssb+, 2 ssb) and sum of its - SSB and three types of double breaks (dsb, dsb+, dsb++) and sum of its -DSB.

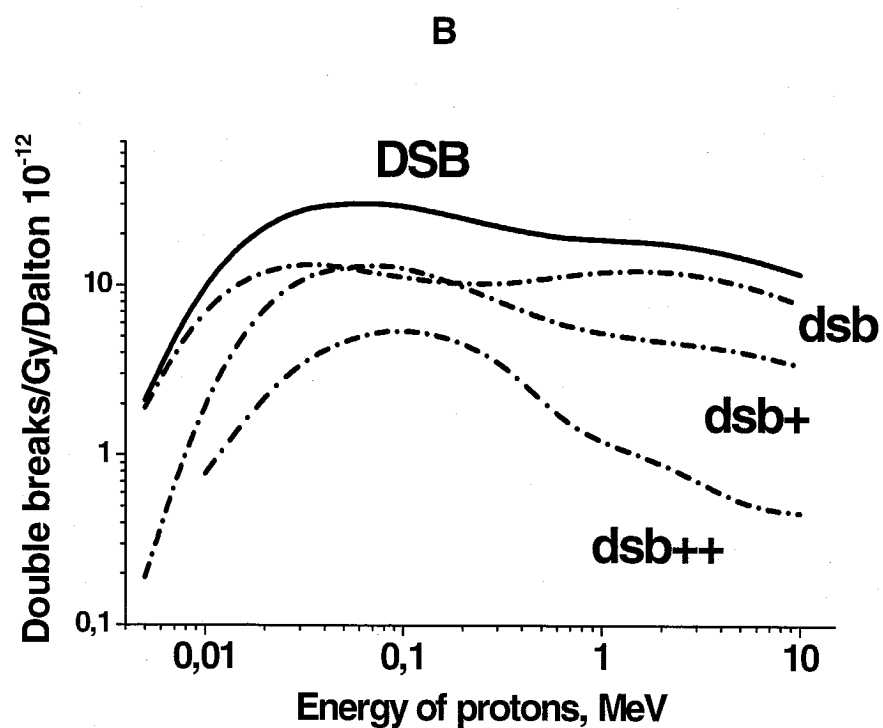
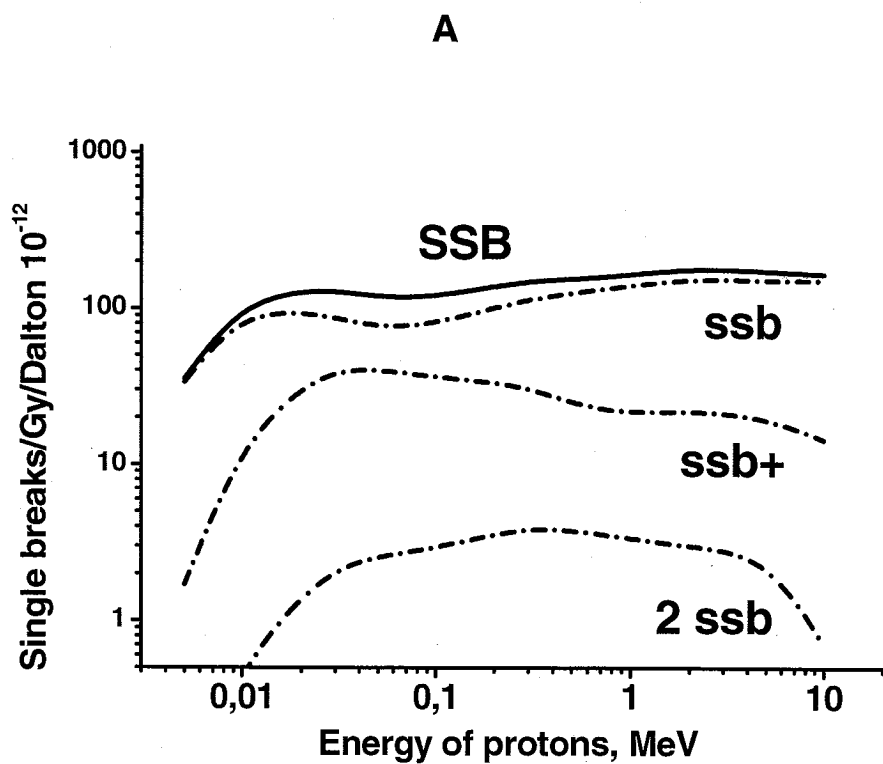


Fig. 7 Simulated yields of DNA breaks: SSB (panel A) and DSB (panel B) classified on complexity and shown as a function of energy of proton affected straightforwardly to the DNA segment.

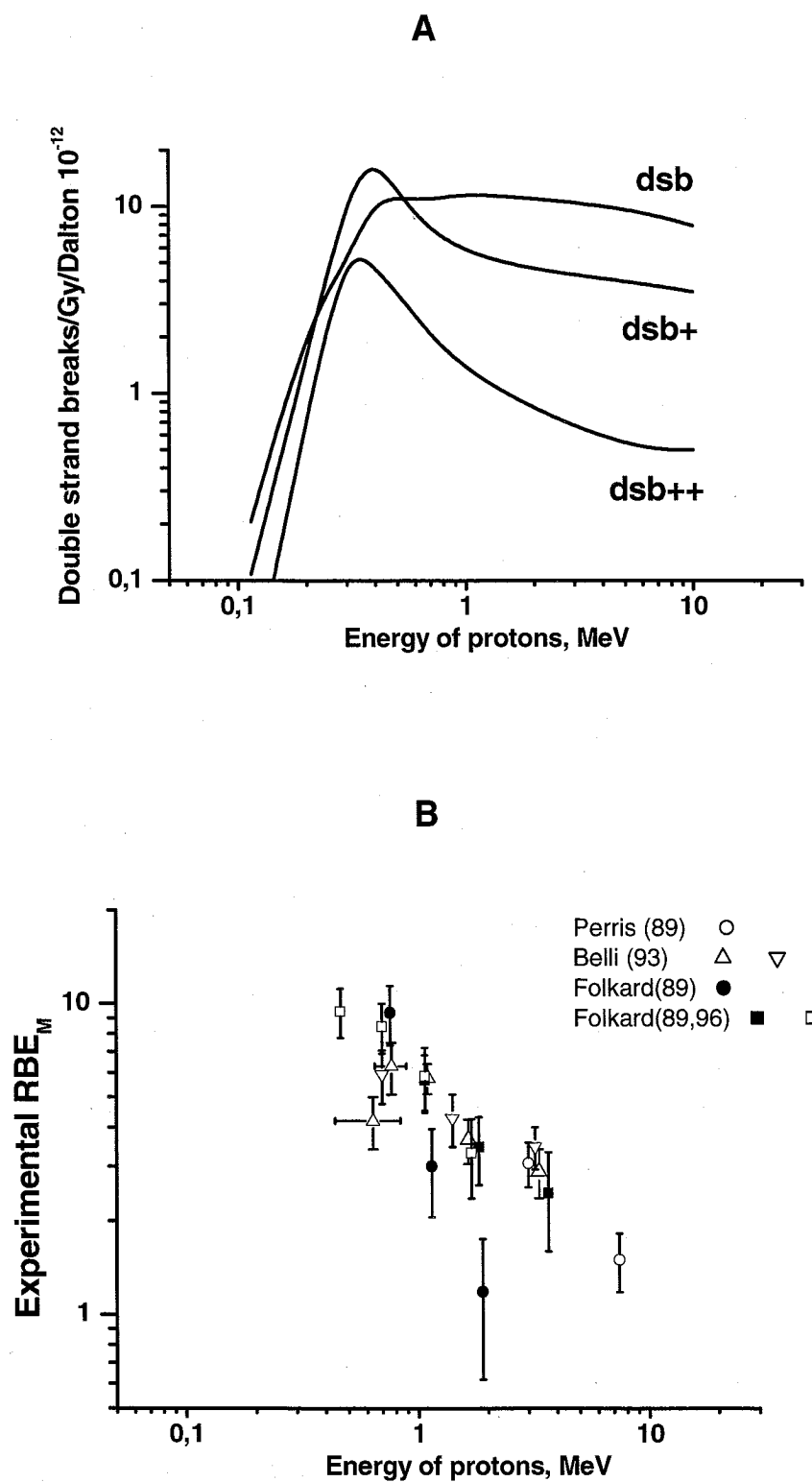


Fig. 8 Calculated double strand breaks in the segment of DNA homogeneously distributed in the cell nuclear (A) in comparison with experimental RBE_M obtained by different researchers (B).

To compare the theoretical yields of DNA damage with experimental data the double strand breaks in DNA segment were extra simulated with averaging on location of target over whole cell nuclear in the geometry shown in fig.1. In this case there is the low-energy threshold of 70 keV for protons to pass 1 μm cytoplasm layer. Besides, for low-energy protons with range much less than geometry chord in cell nuclear the dose distribution is essentially non-homogeneous over the nuclear that just was taken into account in our modeling. In the fig.8, panel A, the yields of DSBs simulated in short DNA segment homogeneously distributed in a cell nuclear are shown as a function of initial energy of protons. It was shown the three types of double breaks: dsb, dsb+ and dsb++. For comparison the experimental data ¹⁶⁻²⁰⁾ are shown in the same figure, panel B. The experimental RBE_M were drawn to match their shapes with simulated values.

Discussion

To analyze the details of V79 cells irradiation by proton beam it was used the description in terms of linear energy 'y'. This value has been recommended by ICRU ⁵⁾ as a tool, more closely related to biological effects of radiation and useful for estimation of RBE values using dose averaged linear energy, y_D ⁵⁾. Considering that linear energy is defined without reference to track structure it remains applicable even if a range of ionizing particle is less than size of a target that was just the case of this statement of the task.

Calculated spectra of linear energy and averaged values using ellipsoid model of cell nuclear, see fig.2-3, obviously show the significant distinction between LET and y_F . This distinction manifests mostly for low-energy protons with ranges comparable or less than a size of target volume. Plotting calculated y_F and y_D as a function of proton energy in the fig. 3 it was found a clear peak at about 550 keV of proton energy. So, the 550 keV protons contribute at average the largest absorbed energy to cell nuclear compared with the rest: above and below proton energy values.

Based on the microdosimetry approach and using the distribution of linear energy in ICRU sphere the quality factor can be calculated as following ⁵⁾. The expected radiation effect with given absorbed dose is governed by the spectra of linear energy this dose was delivered. So, the quality factor $\langle Q \rangle$ is evaluated by averaging on the linear energy distribution with the following formula ⁵⁾.

$$\bar{Q} = \int Q(y) d(y) dy$$

where $d(y)$ is the distribution of absorbed dose in y; $Q(y)$ – is weighting function determined for

1 μm diameter ICRU tissue sphere. The weighting function $Q(y)$ was based in part on observations and theoretical considerations in radiation biology and has been fitted by simple analytic formula in ICRU⁵. The $Q(y)$ shows a peak at linear energy about $140 \text{ keV}/\mu\text{m}$ (LET near $120 \text{ keV}/\mu\text{m}$) and decreases approximately linearly below and above this value.

We used the above formula to calculate quality factor for low energy protons. Substituting in the formula the calculated in this work distributions of absorbed dose, $d(y)$, shown in fig 5, $\langle Q \rangle$ was estimated numerically to 27 and 1.6 for 250 keV and 10 MeV protons respectively.

The distribution of linear energy of 250 keV protons calculated using ICRU sphere, fig.5, extends up to $160 \text{ keV}/\mu\text{m}$. It is interesting to note the following statement. The entering in the target proton with energy 50 keV, which range is about $1 \mu\text{m}$ (full absorption in the ICRU sphere) gives rise the linear energy $75 \text{ keV}/\mu\text{m}$. At that the curve $y d(y)$, shown in fig. 5, has the peak at $140 \text{ keV}/\mu\text{m}$ which is the result of absorption of 93 keV, i.e. much larger full absorption energy. Therefore, so large linear energies can result only from protons with energies around Bragg peak that cross the target along sphere diameter. In other words, the largest linear energies in the ICRU sphere distribution are the result of so called “crossers” (particles crossing the target) but not of the “stoppers” (particles full slowing down inside the target).

A “crossers” are mainly responsible for formation of energy depositions in all the used targets shown in fig. 6 for energies higher 1 MeV. Those energies correspond to ranges that are much higher than target size. In this case effect of δ -rays is relatively small. That is why all the following values: LET, y_F and y_D were found to be approximately equal each other. With further decreasing proton energy, curves show the peaks and a sharp drops at 480 keV and 70 keV for ICRU sphere located in the most distant point (ii) and whole cell nuclear respectively, see fig.6. The reason of such drops is too small ranges of low-energy protons for they to be able pass the cytoplasm before nuclear target. The decreasing left parts of the curves result from protons with ranges about or a bit larger that the distance from base to target which impart small energy of track ends.

It can be seen from fig. 6 the curves for ICRU sphere have the larger slope and peak values compared with the case of cell nuclear. Such distinction is the result of difference in size of the targets. But for the same ICRU sphere and different location inside a cell nuclear – the distinction is due to different pathways needed for proton to reach the target. The range of y_D value extends up to $106 \text{ keV}/\mu\text{m}$ for ICRU sphere and up to $77 \text{ keV}/\mu\text{m}$ for whole cell nuclear respectively. So, at the peaks, y_D value for ICRU sphere is 1.4 higher than for whole cell nuclear. According to definition, y_D value describes the dispersion of linear energy distribution which increases with decreasing the size of target. This can be extra illustrated by comparison of linear energy distributions shown in figs 2 and 5 that relate to peaks shown in fig. 6 at 550 and 250 keV respectively. Indeed, the quotient of maximal by mean ‘y’ values are $106/66 = 1.5$ for cell

nuclear, fig.2, and $165/68 = 2.4$ for ICRU sphere, fig.5, respectively. So that with decreasing the size of a sensitive volume the spread of linear energy goes up.

Fig.7 shows possible types of curve shape for various DNA breaks as a function of proton energy. It can be clearly seen that both sum of all single breaks (SSB) and simple single breaks (ssb) show monotone increasing curves in the range from 70 keV to 10 MeV whilst complex single breaks (ssb+ and 2ssb) show the curve with maximum. The sum of double breaks (DSB) and the complex breaks (dsb+, dsb++) also show the curves with maximum at about 0.2 MeV. The exception is the shape of simple double strand breaks (dsb) see fig.7-b.

In the fig. 8 the calculated complex DSB are shown as a function of initial energy of protons entering a cell. They can be qualitatively compared in curve shapes with experimental values of RBE_M for inactivation/mutation of V79 cells. The presented experimental data are as following. In the papers¹⁶⁻¹⁷⁾ it was studied the RBE_M values of low energy protons with respect to 250 keV X-rays for cell survival using Chinese hamster V79 cell line. They used both proton and deuteron beams to get the highest LET cause given the same energy a deuteron moves about twice slower compared proton, so LET increases. The energy of protons and deuterons was ranged 0.76 – 3.66 MeV. The maximal RBE values were estimated to a ratio of initial slopes of proton and reference dose response curves. The obtained results showed that for survival endpoint RBE_M ranged from 1.18 when cells were exposed to 1.9 MeV protons to about 9.4 for 0.93 MeV deuterons (0.46 Mev/amu).^{*} In the next paper¹⁸⁾ it was investigated the RBE values of low energy protons with respect to ^{60}Co γ -rays for cell survival using V79 cell line. The proton energies were 3.0 and 7.4 MeV. The maximal RBE values estimated to a ratio of initial slopes were 3.1 and 1.5 respectively. In the studies¹⁹⁻²⁰⁾ it was presented the RBE values estimated using survival and mutation endpoints of V79 cells exposed with proton energy ranged from 2.8 to 4.5 MeV. In the paper²⁰⁾ authors have published the correction to previous experimental results¹⁹⁾. They tried to fit dose response data with more proper curve. So, the re-evaluated maximal RBE values were calculated as a ratio of initial slopes and ranged from 1.3 to 5.7²⁰⁾.

To put the data¹⁹⁻²⁰⁾ in fig. 8 the incident proton energy entering a cell were used instead of energy of initial beam or energy in a cell at 3 μm depth as it was used in the original paper. Then, we have to correct the RBE_M values for the lowest-energy protons in the following way. To fit experimental dose response²⁰⁾ they used two different fitting functions: linear quadratic S_1 and parametric regression S_2 , presented below. Then it was assumed that maximal RBE value equals to quotient initial slopes (or alpha coefficients) of proton and reference curves for those two functions. But in the 2nd case the correct estimation of maximal RBE should be calculated using the following formulas.

$$S_1 = e^{-\alpha_p D - \beta_p D^2} \Rightarrow \text{RBE}_{\max} = \frac{\alpha_p}{\alpha_x}$$

$$S_2 = f + (1-f)e^{-\alpha_p D} \Rightarrow \text{RBE}_{\max} = (1-f) \frac{\alpha_p}{\alpha_x}$$

where α_p , β_p , α_x , f – parameters of regression.

So that, the presented in fig.8 RBE_M values were reduced by 6-30% for proton energies 0.04, 0.26, 0.64 and 0.77 MeV compared with RBE_M values presented in the original paper²⁰⁾.

**Note. The misprint in the table 4 of Folkard et al¹⁷⁾ was remedied.*

The results of this paper show the following specific points. The most suitable for delivering absorbed energy in whole V79 cell nuclear are the protons with incident on a cell energy of 550 keV. At that the protons with 400 keV were found to be the most efficient to induce a complex double strand breaks of DNA over a cell nuclear averaged. Comparing 400 keV protons with respect to 10 MeV protons it was found 9 and 5 fold for dsb++ and dsb+ respectively. Those calculated numbers mainly are in the range of experimental RBE_M values shown in the fig. 8, right panel. The rest of examined types of DNA breaks obviously do not correlate with the experimental data. In general, results of this paper agree well with the following statements: (i) sensitive sites for cell lethality (transformation) are located in the cell nuclear and (ii) the complex DSB are the most relevant initial lesions leading to cell killing or transformation.

Conclusions

The results of biophysical modeling of initial events in the nuclear of V79 cells by protons have been presented. The key points of the model are as following (1) a proton stochastic track structure was simulated by Monte Carlo algorithm followed protons from initial energy to full local absorption; (2) the biological target was constructed based on morphological data of V79 cells and ICRU sphere in terms of linear energy; (3) complex DNA double strand breaks were assumed to be a crucial lesions leading to cell killing or transformation. It was not introduced extra adjustable parameters or fitting procedure in order to compare with experimental data on cell survival/mutation. Instead, the relative fold of biophysical parameters such as dose averaged linear energy and complex DNA double strand breaks were considered.

The main results of this paper obtained for V79 cells can be illustrated in fig. 3 and fig. 8. It can be seen that: (i) dose averaged, y_D , values as a function of proton energy has a single peak at 550 keV; (ii) the peak value is larger for local sub-nuclear sensitive volume than for whole cell nuclear (iii) in the spectrum of DNA breaks only complex DSB can correlate with experimental data on RBE_M . These findings are in reasonable agreement with

inactivation/mutation data using V79 cells published by different research groups¹⁶⁻²⁰. It should be pointed out that our calculations are the results of parameter-free simulation. The main results of this paper showed that local energy deposition in cell nuclear and clustered ionizations in DNA should play an important role in the formation of radiation biological effect.

References

1. Robertson J.B. et al (1975) Radiobiological studies of a high energy modulated proton beam utilizing cultured mammalian cells. *Cancer*. **35**: 1664-1677.
2. NCRP (1990) The relative biological effectiveness of radiation of different quality. NCRP Report 104. National Council on Radiation Protection and Measurements, Bethesda, Maryland, USA.
3. Geard C.R. (1996) Neutron induced recoil protons of restricted energy and range and biological effectiveness. *Health Phys.* **70**: 804-811.
4. Raju M.R. (1995) Proton radiobiology, radiosurgery and radiotherapy. *Int. J. Radiat. Biol.* **67**: 237-259.
5. ICRU (1986) The quality factor in Radiation Protection, ICRU Report 40. International Commission on Radiation Units and Measurements, Bethesda, Maryland, USA.
6. ICRP (2003) Relative Biological Effectiveness (RBE), Quality factor (Q), and radiation weighting factor (w_R). ICRP Publication 92, Ann. ICRP 33 (4).
7. ICRP (1991) Recommendations of the International Commission on Radiation Protection, ICRP Publication 60, Ann. ICRP 21 (1-3).
8. Lett J.T. (1992) Damage to cellular DNA from particulate radiations, the efficacy of its processing and the radiosensitivity of mammalian cells. *Radiat. Environ Biophys* 31: 257-277.
9. Ward J.F. (1995) Radiation mutagenesis: the initial DNA lesions responsible. *Radiat. Res.* **142**: 362-368.
10. Ottolenghi A., Monforti F. and Merzagora M. (1997) A Monte Carlo calculation of cell inactivation by light ions. *Int. J Radiat. Boil.* 72: 505-513.
11. Uehara S., Toburen L.H. and Nikjoo H. (2001) Development of a Monte Carlo track structure code for low-energy protons in water. *Int. J Radiat. Boil.* 77: 139-154.
12. Nikjoo H., O'Neil P., Terrisol M. and Goodhead D.T. (1999) Quantitative modeling of DNA damage using Monte Carlo track structure. *Radiat. Environ. Biophysics.* **38**: 31-38.
13. Wilson W.E., Miller J.H. and Nikjoo H. (1994) PITS – A code system for Positive Ion Track Structure. *Computational approach in Molecular Radiation Biology*. M.N. Varma and A. Chatterjee (eds.). Plenum Press. New York. 137-154, 1994.

14. Nikjoo H, Uehara S, Wilson W.E., Hoshi M. and Goodhead D.T. (1998) Track structure in radiation biology: theory and applications. *Int. J. Radiat. Biol.* **73**: 355-364.
15. Nikjoo H, Uehara S, Khvostunov I.K., Cucinotta F.A., Wilson W.E. and Goodhead D.T. (2001) Monte Carlo track structure for radiation biology and space applications. *Phys Med.* **17** Suppl 1: 38-44.
16. Folkard M. et al. (1989) The irradiation of V79 mammalian cells by protons with energies below 2 MeV. Part I. Experimental arrangement and measurements of cell survival. *Int. J. Radiat. Biol.* **56**: 221-237.
17. Folkard M. et al. (1996) Inactivation of V79 cells by low-energy protons, deuterons and helium-3 ions. *Int. J. Radiat. Biol.* **69**: 729-738.
18. Perris A. et al (1986) Biological effectiveness of low energy protons. I. Survival of Chinese hamster cells. *Int. J. Radiat. Biol.* **50**: 1093-1101.
19. Belli M. et al. (1989) RBE-LET relationship for the survival of V79 cells irradiated with low energy protons. *Int. J. Radiat. Biol.* **55**: 93-104.
20. Belli M. et al. (1993) Inactivation and mutation induction in V79 cells by low energy protons: re-evaluation of the results at the LNL facility. *Int. J. Radiat. Biol.* **63**: 331-337.
21. Datta R., Cole A. and Robinson S. (1976) Use of track-end alpha particles from ²⁴¹Am to study radiosensitive sites in CHO cells. *Radiat. Res.* **65**: 139-151.
22. Townsend K.M.S. and Marsden S.J. (1992) Nuclear area measurements on viable cells, using confocal microscopy. *Int J Radiat. Biol.* **61**: 549-551.
23. ICRU (1983) Microdosimetry, ICRU Report 36. International Commission on Radiation Units and Measurements, Bethesda, Maryland, USA
24. Watt D.E., 1996, Quantities for dosimetry of ionising radiations in liquid water / Reference Book / Taylor & Francis Ltd., 1 Gunpowder Square, London EC4A 3DE, 1996, 422 P.